Research report: Comparison of different time-frequency representations.

Mariia Fedotenkova, Axel Hutt

Research report: Comparison of different time-frequency representations.

Mariia Fedotenkova[1] and Axel Hutt

INRIA Nancy Grand-Est, team NEUROSYS, Villers-lés-Nancy, France

December 8, 2014

[1]mariia.fedotenkova@inria.fr

Contents

Chapter 1

Introduction

Time-frequency representation (TFR) is analysis methods which expands stationary spectral analysis to non-stationary cases. It is used for distinguishing different frequency components presented in the signal as well as their evolution in time.

This report compares different time-frequency representations based on previous studies (see [2], [4] and [6]) and implementations (see [3]) but in application to EEG data analysis. This work compares several time-frequency representations taking into account speed, accuracy and localization of each method and chooses the best one for the particular problem. The methods discussed in this report are:

- Short-time Fourier transform and spectrogram (STFT);
- Continuous Wavelet transform and scalogram (CWT);
- Wigner-Ville distribution;
- Choi-Williams distribution;
- Reassigned spectrogram.

The comparison was held on two test data sets and afterwards the winning TFR was applied to the real data.

Chapter 2

Overview of time-frequency representations

First step of the analysis was held on the test data presented by sum of sines for all studied time-frequency representations.

2.1 Test data description

Test signal is a sum of oscillations with three different frequencies appearing at different times. It is presented on Fig.2.1. This chapter describes the data used for the first step of the analysis and also gives an overview of methods used to obtain time-frequency representations.

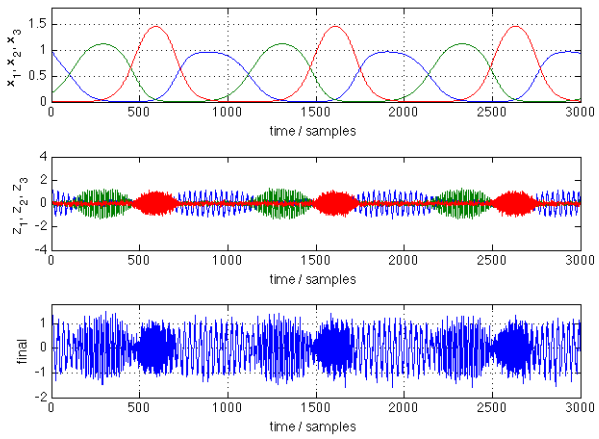

Figure 2.1: Test signal `final`.

Original data consist of sum of three signals, which are solution of Lotka-Voltera equations with added high-amplitude oscillations on peak values and small noise oscillations elsewhere ($\sigma = 0.1$). It is of the form:

$$\begin{cases} z_1 = I_1 sin(\omega_1^2 t) + \xi, & \omega_1 = 2\pi \cdot 0.4 \\ z_2 = I_2 sin(\omega_2^2 t) + \xi, & \omega_2 = 2\pi \cdot 0.6 \\ z_3 = I_3 sin(\omega_3^2 t) + \xi, & \omega_3 = 2\pi \cdot 1 \end{cases}$$

where I is the term, which amplifies oscillations at peak values of the solution of Lotka-Voltera system; ξ is a noise term ($\sigma = 0.1$); ω is angular frequency (in rad). Frequency in Hz can be derived as follows:

$$sin(2\pi f_1 t) = sin(\omega_1^2 t) = sin(2\pi(2\pi \cdot 0.4^2)t) \Rightarrow f_1 = 2\pi \cdot 0.4^2$$

and

$$\begin{cases} f_1 = 2\pi \cdot 0.4^2 &= 1.0053 \\ f_2 = 2\pi \cdot 0.6^2 &= 2.2619 \\ f_3 = 2\pi \cdot 1^2 &= 6.2832 \end{cases}$$

Those frequencies can be seen from PSD of each signal on the fig.2.2.

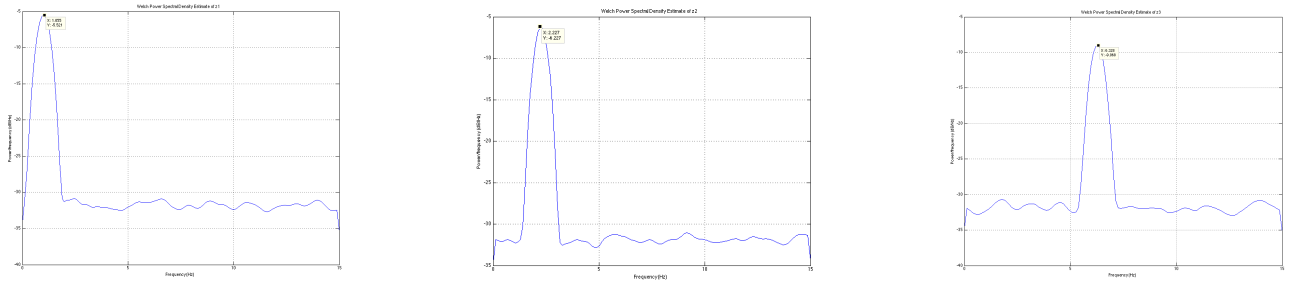

(a) z_1 (b) z_2 (c) z_3

Figure 2.2: Power spectrums of signals z_1, z_2, z_3.

Times at which those oscillations appears can be seen in the following table. Time periods were estimated from x_1, x_2 and x_3 signals, where they are above **50%-level** (since the oscillations appear when those signals are high enough).

Signal	**Times (in samples)**			**Times (in seconds)**		
z_1	$1-109$	$707-1124$	$1726-2144$	$0-3,6$	$23,6-37,5$	$57,5-71,5$
			$2749-3000$			$91,6-100$
z_2	$107-464$	$1123-1481$	$2143-2503$	$3,6-15,5$	$37,4-49,4$	$71,4-83,4$
z_3	$458-721$	$1475-1740$	$2496-2763$	$15,3-24$	$49,2-58,0$	$83,2-92,1$

With known frequency and times at which they appear the ideal time-frequency representation can be constructed (see fig.2.3). In addition small amount of blur was added.

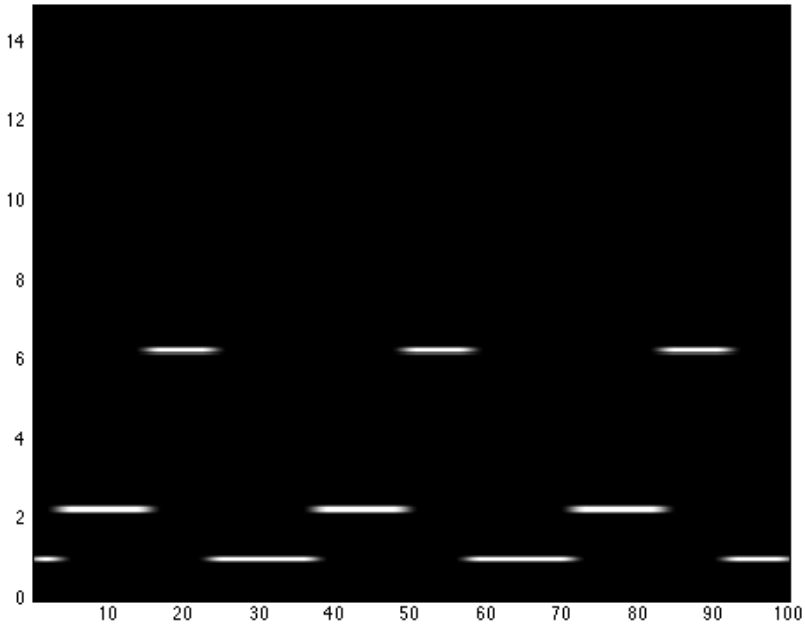

Figure 2.3: Ideal TFR.

2.2 Time-frequency distributions

1. **Short-time Fourier transform and spectrogram**
   Short-time Fourier transform (STFT) is windowed fourier transform obtained with window sliding along the signal, thus providing a matrix (time × frequency) instead of a vector (frequency) obtained with a normal Fourier transform. Spectrogram is squared values of STFT. On fig.2.4, first two plots are obtained with Matlab routine. Left picture represents a power spectral density (PSD) in a logarithmic scale: $10 \cdot \log_{10}(|PSD|)$. Plotting only absolute values of PSD provides better readability (middle and right figures). Right picture is obtained using Time-Frequency Toolbox (TFTB) [3] and gives more smoothed results, tough slightly more blurred. Spectrogram obtained with TFTB of the size 300×3000, while for TFR computed with MATLAB it is only 300×22. It happens because MATLAB returns vector of time as points where the spectrogram was computed (window location). In both cases Hanning window of length 256 was used.

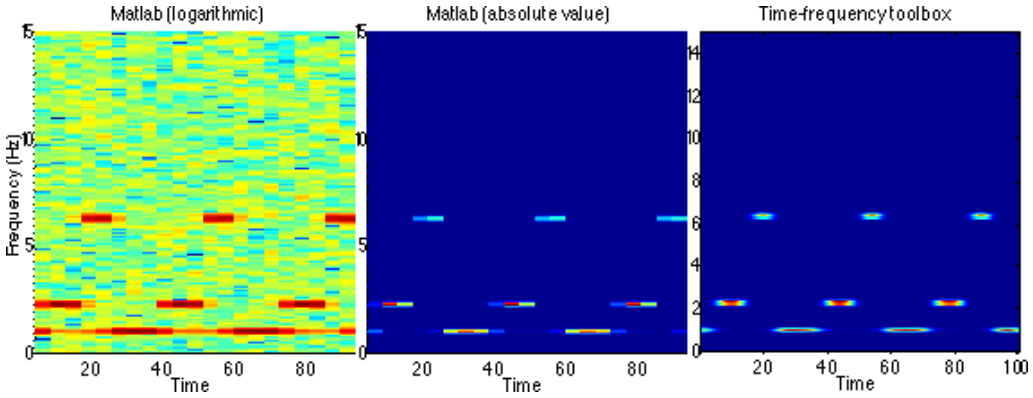

Figure 2.4: Spectrograms.

2. **Continuous wavelet transform and scalograms**
   Similarly with STFT and spectrogram, scalogram is squared value of continuous wavelet transform (CWT) ([1], [7]). On fig.2.5, the left picture is a real Morlet wavelet, the middle one is 4^{th} derivative of complex Gaussian and the right one is a complex Morlet with center frequency 0.95 and **bandwidth parameter 2**. Complex wavelets give more smoothed results because they include both real and imaginary parts, which gives broader peaks.

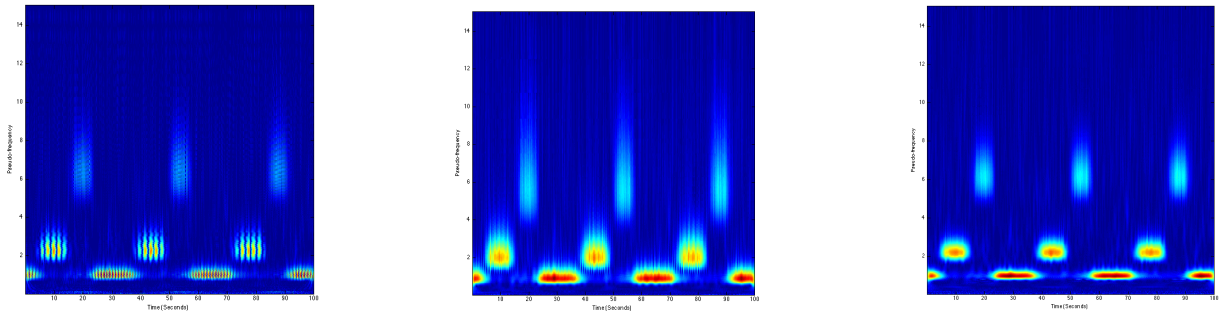

(a) Morlet (b) Complex Gaussian (c) Complex Morlet

Figure 2.5: Continuous Wavelet transform.

Wavelet transforms (and scalograms accordingly) were computed for frequencies $\mathbf{0.05}, \mathbf{0.1}, \ldots, \mathbf{15}$ and corresponding scales.

Two different approaches to WT were used. One is using **convolution**: each row of TFR is obtained by convolving the signal with the wavelet at a particular scale. Another approach is

based on **fast Fourier transform (FFT)**: it applies FFT to both the wavelet and the signal, takes the product of those two in frequency domain and then inverts it back to time domain. See examples of CWTs obtained with convolutions and FFT (for complex Morlet wavelet) as well as plots of their frequency-scale correspondence on fig.2.6.

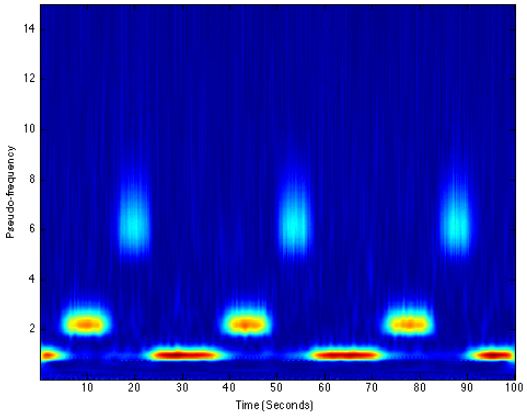

(a) CWT using convolution

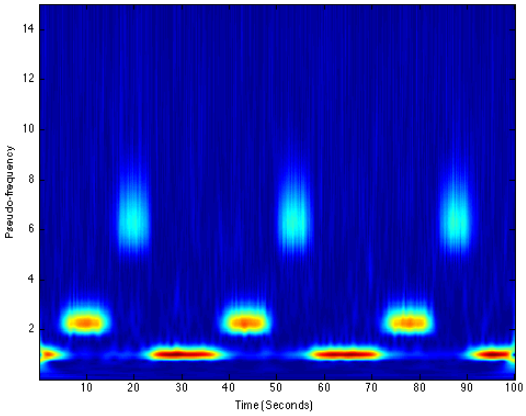

(b) CWT using FFT

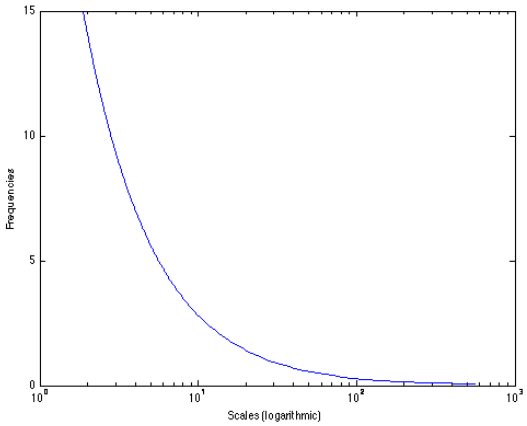

(c) Scale-frequency plot (convolution)

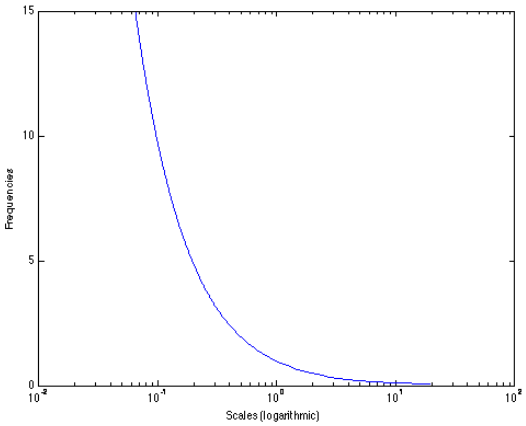

(d) Scale-frequency plot (FFT)

Figure 2.6: Comparison of wavelet transforms obtained with convolution and FFT.

The CWT using FFT introduces distortions on the edges of TFR meanwhile it eliminates artifacts at low frequencies ≈ 0 Hz.

Analogically to STFT and Spectrogram (squared modulus of STFT), **Scalogram** is connected to CWT by quadratic relation and it represents the percentage of energy for each CWT coefficient. Fig.2.7 shows an example of scalogram obtained with complex Morlet wavelet. It provides better readability and reduces noise components. In further analysis only scalogram will be used instead of wavelet transform.

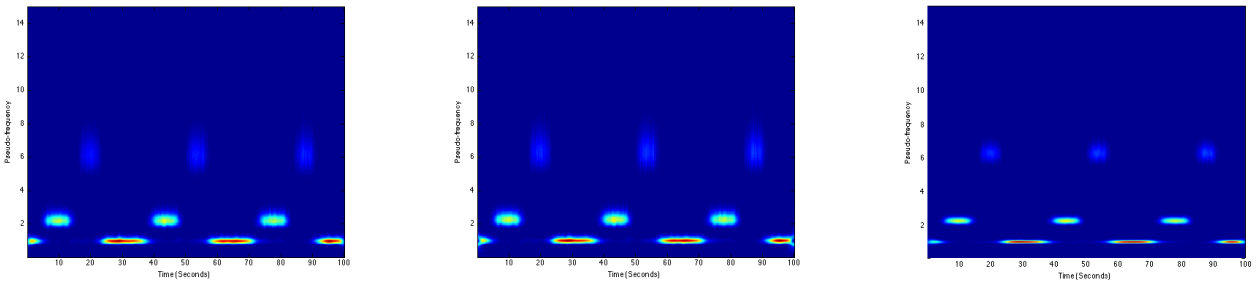

(a) Using convolution (b) Using FFT (c) Using TFTB

Figure 2.7: Scalograms obtained with different techniques.

3. **Wigner-Ville distribution**
   On fig.2.8, Wigner-Ville distribution (WVD) gives a lot of interference terms (see left image). Pseudo WVD (smoothed in frequencies) reduces those terms, but still not enough (middle image). Smoothed pseudo WVD (smoothing of WVD both in time and frequency) gives good results but requires a lot of time for computations.

   To obtain these representation analytical signal was used. It was obtained from original signal using `hilbert` MATLAB function. It was done due to the fact that with discrete WVD aliasing may appear at half of Nyquist frequency (in contrast to Fourier transform).

   In addition, 1%-thresholding was applied to these TFRs. It was done, because WVD gives negative values (see fig.2.9). **In order to perform comparison with known TFR those negative components were truncated** (see fig.2.8).

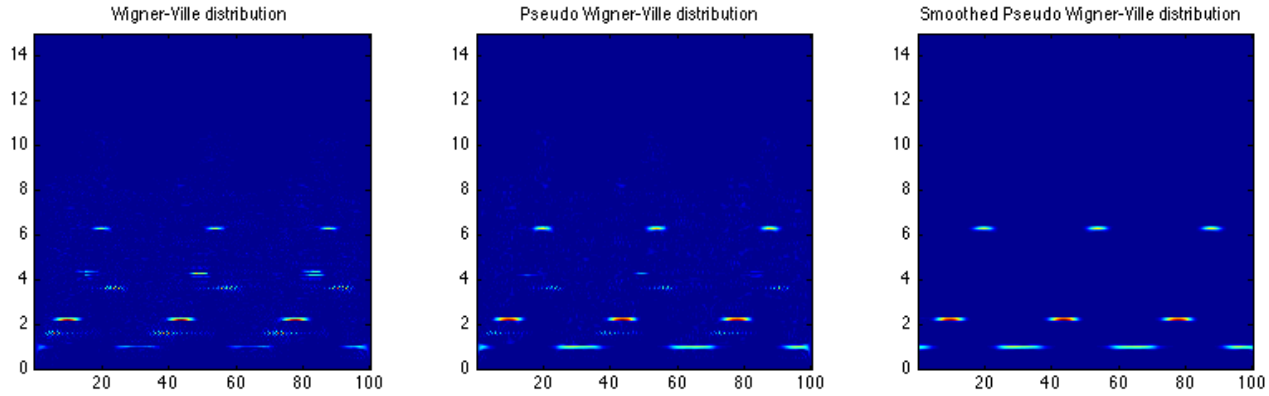

Figure 2.8: Wigner-Ville distributions after eliminating negative components.

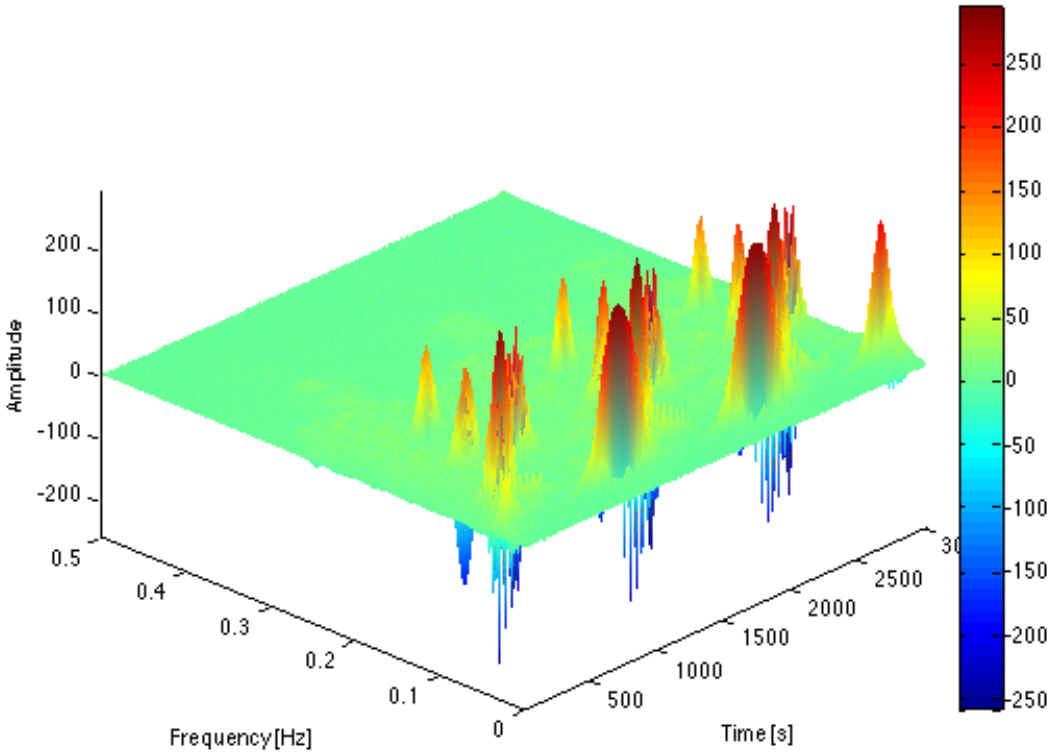

Figure 2.9: Wigner-Ville distribution with negative components.

4. **Choi-Williams distribution**
   On fig.2.10, Choi-Williams distribution (CW) also provides good results but as well time consuming. Interference terms also can appear depending on the signal characteristics.

   As well as in WVD Choi-Williams distribution requires use of analytical signal and **truncation of negative components**.

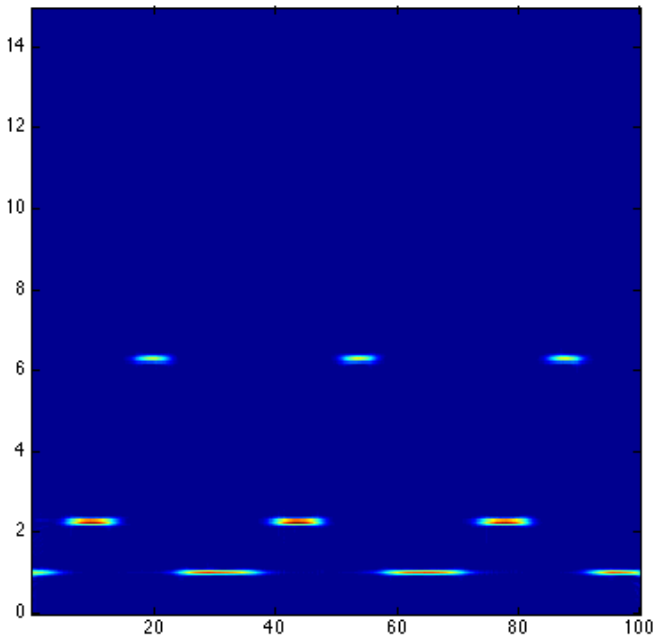

Figure 2.10: Choi-Williams distribution.

5. **Reassigned spectrogram**
   The idea of spectrogram reassignment is that spectrogram is seen as mass distribution and the total mass assigned not to geometrical center but rather to center of gravity. For comparison

normal (fig.2.11., left) and reassigned (fig.2.11., right) spectrograms are shown. Eliminates all noise components, probably not suitable for EEG

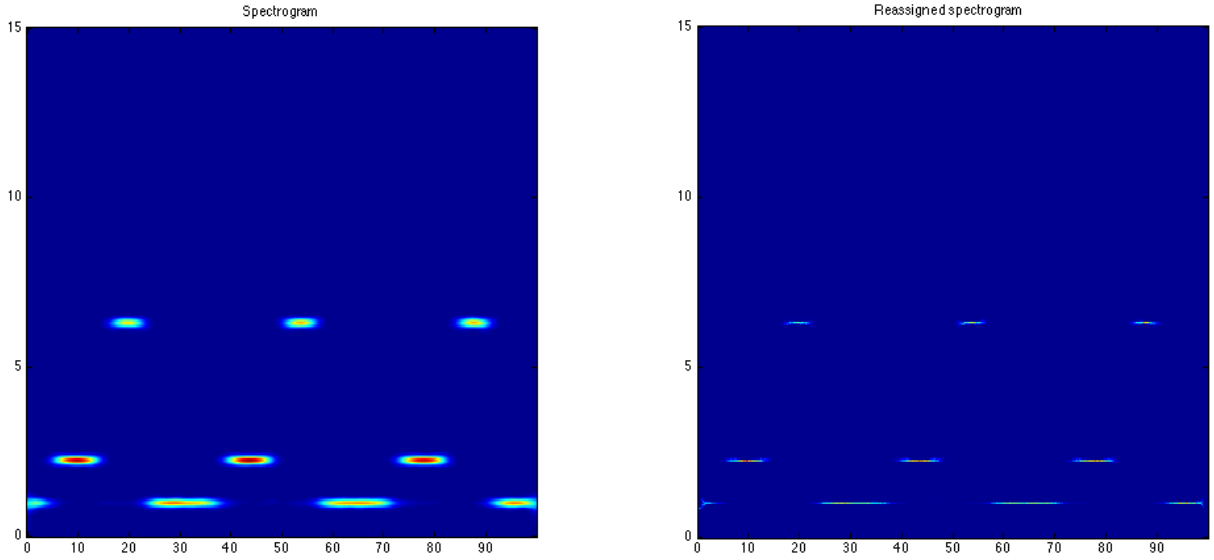

Figure 2.11: Spectrogram reassignment.

This chapter provided overview of existing time-frequency methods and further chapter will summarize the quantitative analysis of the latter.

Chapter 3

Comparison of time-frequency representations

3.1 Quantitative comparison of all methods

To quantitatively compare different TFRs different approaches were used. The first method is to measure classification error as difference between estimated TFR and ideal representation. To do so, firstly, they were 0-1 normalized, where white color (1) means presence of frequency component and black (0) - absence. Than ideal TFR was subtracted from the analyzed one. In resulting matrix, if element equals 0 it means the classification is correct, if it is positive - false detection and if it is negative - missed component. Example of those matrices can be seen on fig. 3.1. Then amount of zero (N_c), positive (N_f) and negative (N_m) elements were calculated as a percentage of all matrix elements.

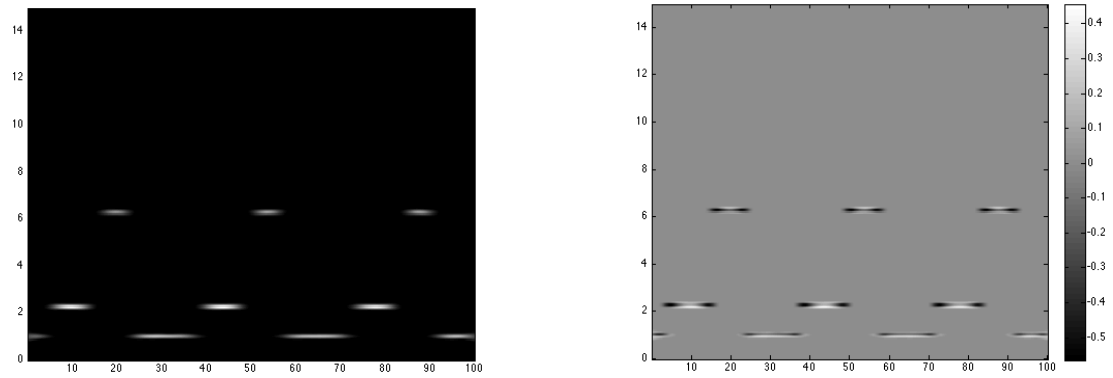

(a) Normalized TFR

(b) Differences between ideal and estimated TFRs

Figure 3.1: Spectrograms obtained with TFTB and its differences with the ideal TFR.

Next criterion is a *mean squared error (MSE)* [8] between two TFRs, given in percents:

$$MSE = \frac{\|I_{es} - I_{id}\|^2}{N} * 100,$$

where I_{es} is an estimated TFR, I_{id} is the ideal TFR and N is the number of elements in TFR.

Three next parameters are taken from [5]. They are:

- The *two-dimensional correlation* between images ρ;
- The *Instantaneous frequency correlation IF*;

- The *Time-frequency resolution measure res.*

For the first two parameters 1.00 means best quality of estimated representation, while for the third one it is 0.00.

All of this criteria for each method are presented in Table 3.1. For scalogram FFT-based method was used, since it slightly faster than one based on convolution, also **to perform the comparison 3%-threshold was used**.

Table 3.1: Performance measures for each method

	N_c	N_f	N_m	MSE	ρ	IF	res
Spectrogram (Matlab)	97.59	1.51	0.89	0.103	0.865	0.744	0.0002
Spectrogram (TFTB)	97.21	1.63	1.16	0.096	0.865	0.715	0.0002
Scalogram (C.Morlet, FFT)	91.21	7.70	1.08	0.360	0.605	0.360	0.0016
WVD	77.8	20.56	1.64	0.215	0.662	0.212	0.0008
pWVD	79.34	19.27	1.39	0.123	0.824	0.257	0.0009
spWVD	97.01	1.63	1.36	0.088	0.888	0.716	0.0001
CWD	96.30	2.33	1.36	0.089	0.885	0.629	0.0001
Reass. Spectrogram	57.81	40.44	1.74	0.250	0.648	0.133	0.0001

Also average computational time was measured for all of the representation (see Table 3.2).

Table 3.2: Computational times for each method

Spectrogram (Matlab)	**Spectrogram (TFTB)**	**CWT (Morl.)**	**CWT (C. Gaus.)**	**CWT (C. Morl.)**
0.160	0.103	0.228	0. 222	0.322

Scalogram (Morl.)	**Scalogram (C. Gaus.)**	**Scalogram (C. Morl.)**	**Scalogram (TFTB)**
0.233	0.229	0.329	6.007

WVD	**pWVD**	**spWVD**	**CWD**	**Reas. Spectro.**
0.118	0.119	16.280	16.282	6.849

3.2 Comparison for different noise levels

The previous data had the standard deviation of noise $\sigma = 0.1$. The following data has higher noise level, but the same TFR. Figures 3.2 and 3.7 shows the signals under study in a time space ($\sigma = 0.3$ and $\sigma = 0.5$ accordingly), figures 3.3 – 3.6 shows estimated TFRs for the signal with $\sigma = 0.3$ and figures 3.8 – 3.11 for $\sigma = 0.5$, finally, Tables 3.3 and 3.4 give estimation of performance measures for both signals.

3.2.1 $\sigma = 0.3$

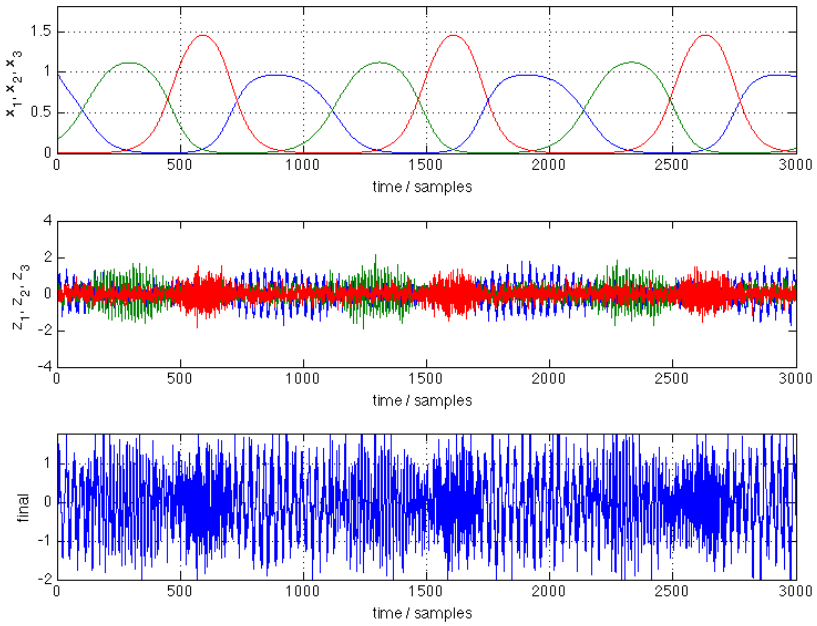

Figure 3.2: Test signal with higher noise level ($\sigma = 0.3$).

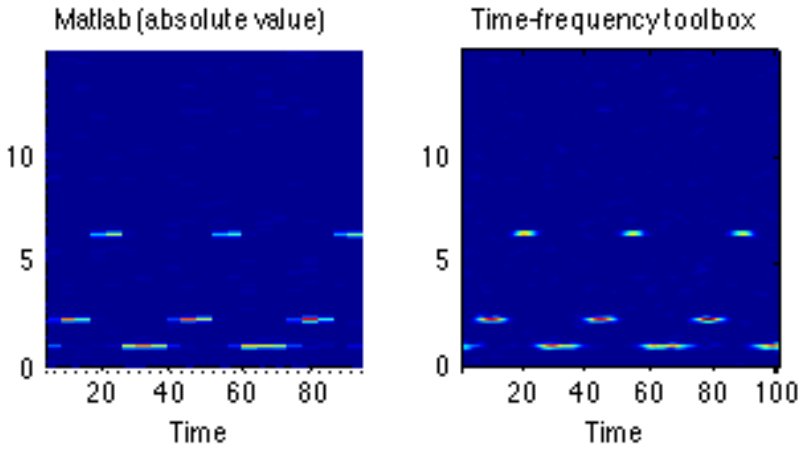

Figure 3.3: Spectrograms ($\sigma = 0.3$).

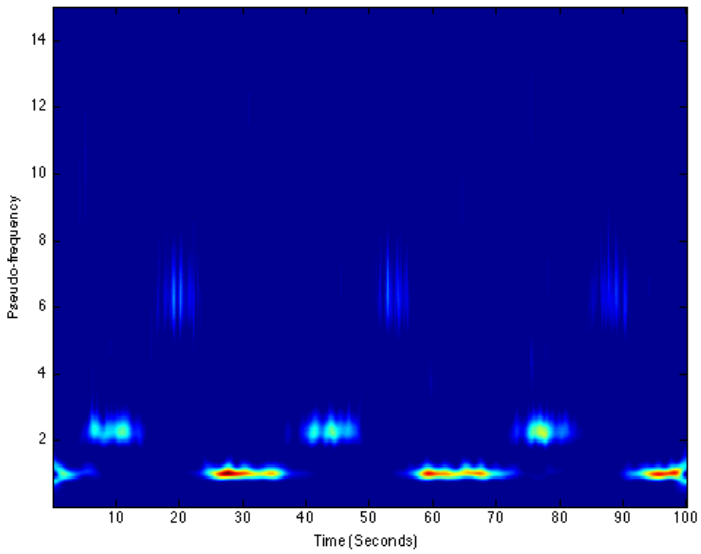

Figure 3.4: FFT-based scalogram using complex Morlet wavelet ($\sigma = 0.3$).

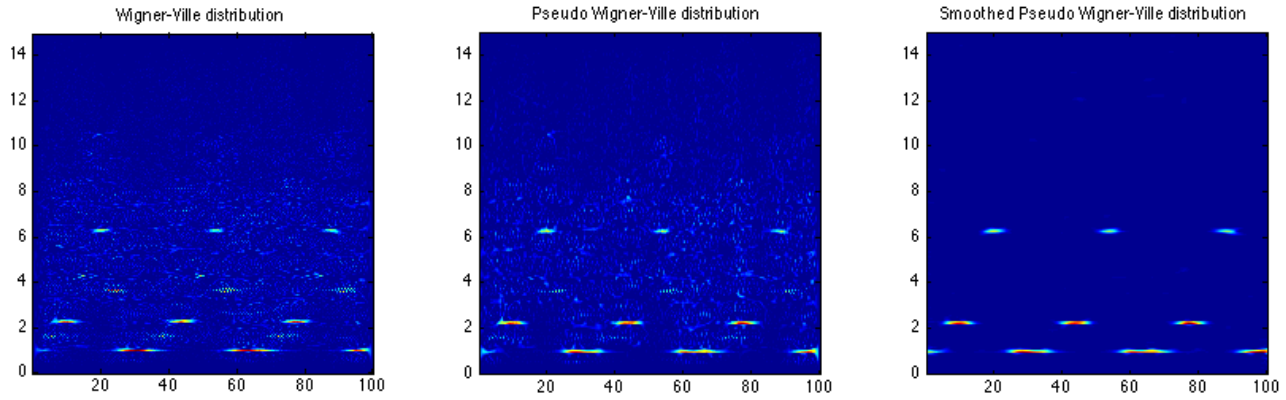

Figure 3.5: Wigner-Ville distributions ($\sigma = 0.3$).

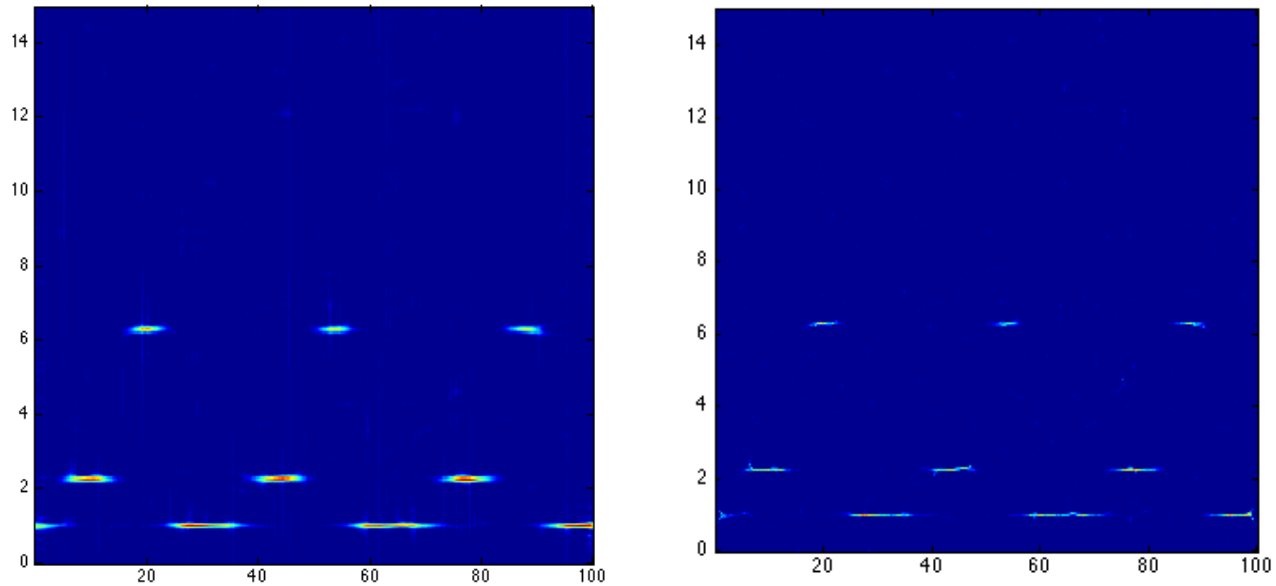

(a) Choi-Williams distribution

(b) Spectrogram reassignment

Figure 3.6: Choi-Williams distribution and Spectrogram reassignment ($\sigma = 0.3$).

Table 3.3: Performance measures for each method with higher noise level ($\sigma = 0.3$)

	N_c	N_f	N_m	MSE	ρ	IF	res
Spectrogram (Matlab)	83.68	15.48	0.83	0.107	0.859	0.286	0.0013
Spectrogram (TFTB)	82.27	16.68	1.05	0.104	0.857	0.309	0.0010
Scalogram (C.Morlet, FFT)	88.82	9.96	1.22	0.312	0.580	0.321	0.0013
WVD	58.98	39.42	1.6	0.348	0.496	0.149	0.0038
pWVD	57.93	40.69	1.37	0.276	0.631	0.176	0.0044
spWVD	87.57	11.07	1.34	0.093	0.876	0.347	0.0005
CWD	78.37	20.26	1.36	0.098	0.867	0.258	0.0005
Reass. Spectrogram	57.83	40.43	1.74	0.253	0.649	0.122	0.0002

3.2.2 $\sigma = 0.5$

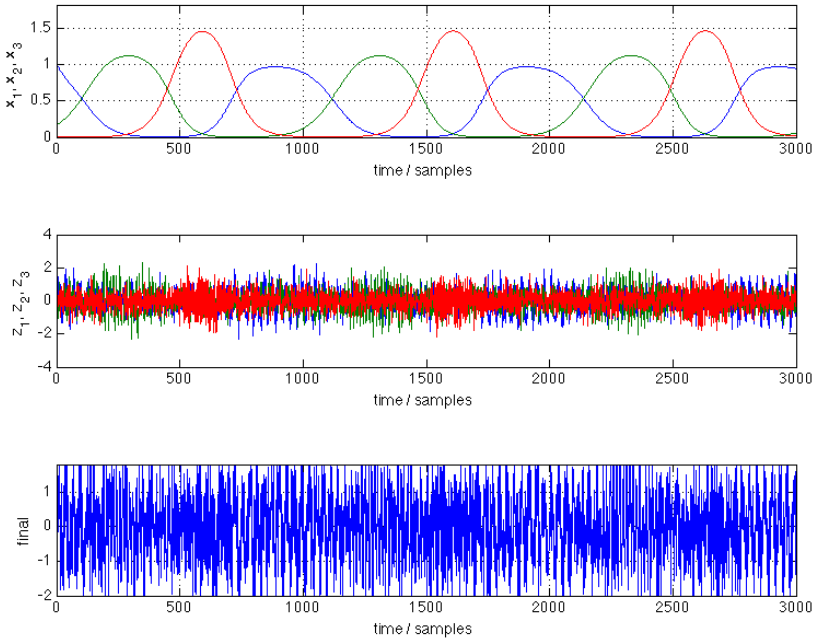

Figure 3.7: Test signal with higher noise level ($\sigma = 0.5$).

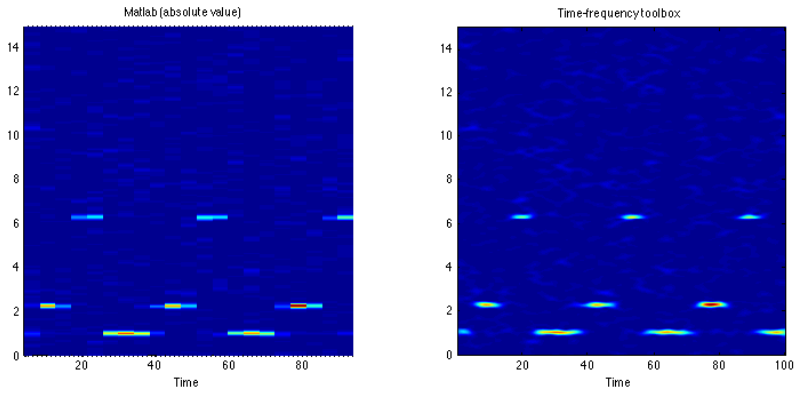

Figure 3.8: Spectrograms ($\sigma = 0.5$).

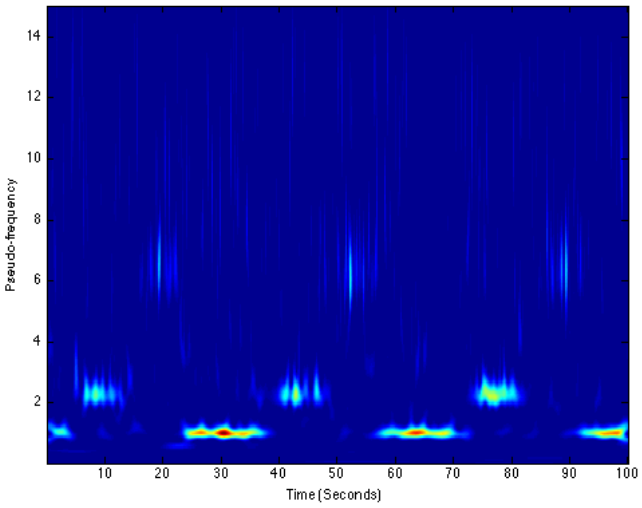

Figure 3.9: FFT-based scalogram using complex Morlet wavelet ($\sigma = 0.5$).

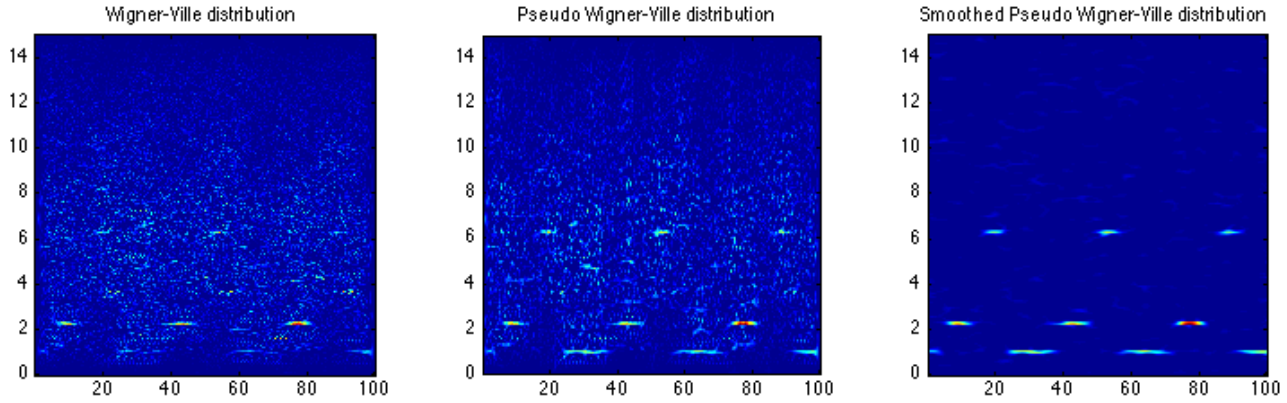

Figure 3.10: Wigner-Ville distributions ($\sigma = 0.5$).

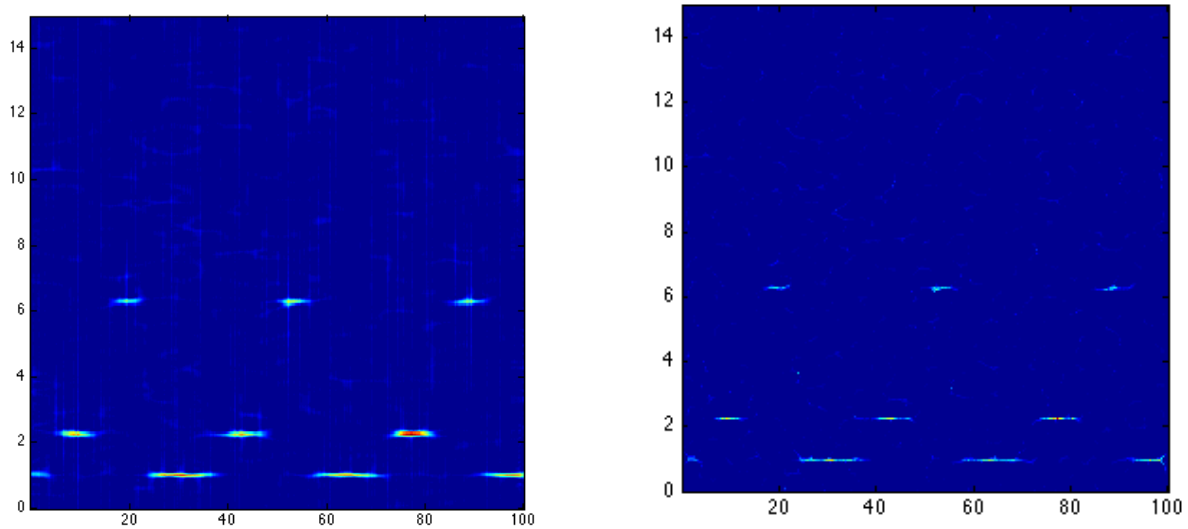

(a) Choi-Williams distribution

(b) Spectrogram reassignment

Figure 3.11: Choi-Williams distribution and Spectrogram reassignment ($\sigma = 0.5$).

Table 3.4: Performance measures for each method with higher noise level ($\sigma = 0.5$)

	N_c	N_f	N_m	MSE	ρ	IF	res
Spectrogram (Matlab)	59.65	39.38	0.97	0.136	0.820	0.182	0.0039
Spectrogram (TFTB)	57.58	41.19	1.23	0.121	0.827	0.197	0.0033
Scalogram (C.Morlet, FFT)	73.57	25.15	1.27	0.327	0.549	0.212	0.0031
WVD	53.26	45.15	1.59	0.679	0.320	0.138	0.0082
pWVD	52.31	46.23	1.45	0.577	0.414	0.158	0.0091
spWVD	67.68	30.89	1.43	0.121	0.845	0.208	0.0019
CWD	62.39	36.15	1.46	0.134	0.817	0.190	0.0017
Reass. Spectrogram	57.42	40.85	1.73	0.273	0.606	0.118	0.0003

3.3 Signal with frequency modulations

This section introduces new test data set and also uses for the analysis only two leading methods: *Scalogram* and *Reassigned spectrogram.*

3.3.1 Test data

The first half of the analyzed signal consists of sum of two sine waves with equal amplitudes but different frequencies (3 and 5 Hz) and the second part consists of sinusoidal frequency modulation, where frequency changes from 3 to 8 Hz in accordance with sine function. Then white noise with different standard deviations ($\sigma = 0.1, 0.3, 0.5$) was added to the signal forming three different test signals. This section, as mentioned above, considers only scalogram (obtained using FFT, complex Morlet) and reassigned spectrogram. The signals in the time domain with different noise levels and its corresponding TFR can be seen on fig.3.13 and fig.3.12. Reassigned spectrograms and scalograms for the signals with different noise levels can be seen on the fig.3.14 - 3.16 and quantitative comparison in the tab.3.5.

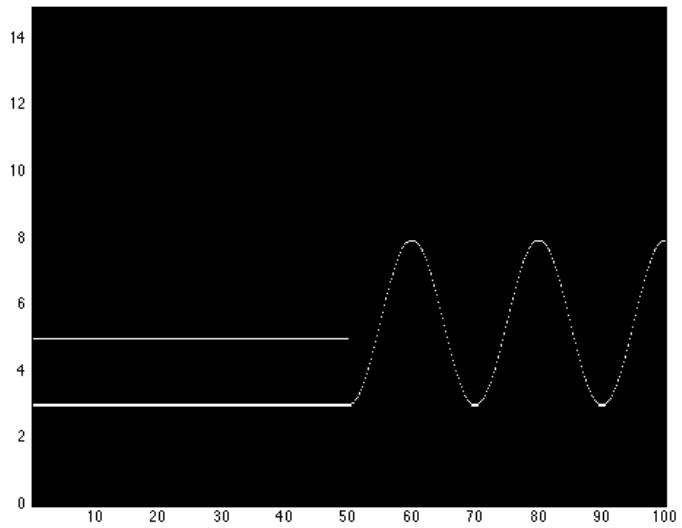

Figure 3.12: Ideal time-frequency representation for the test signal.

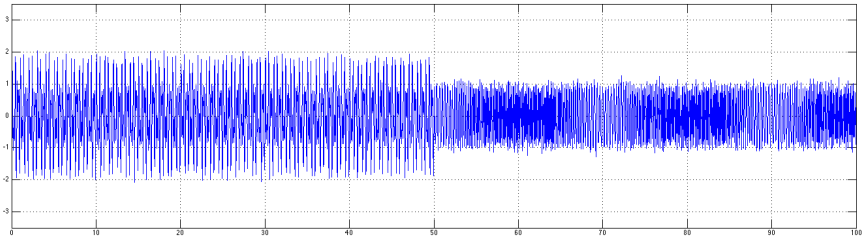

(a) $\sigma = 0.1$

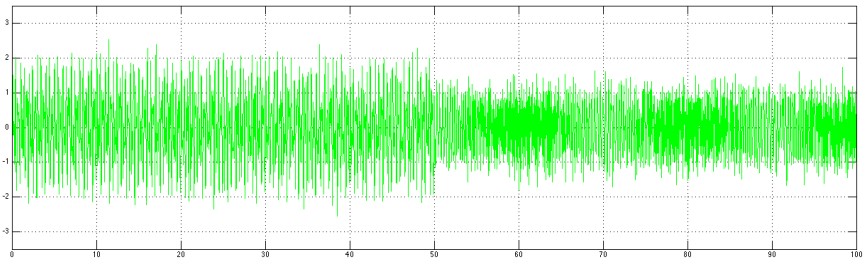

(b) $\sigma = 0.3$

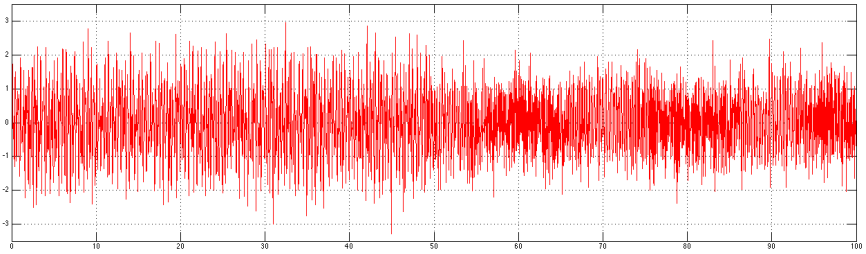

(c) $\sigma = 0.5$

Figure 3.13: The signals in the time domain with different noise levels.

3.3.2 Results for different noise levels

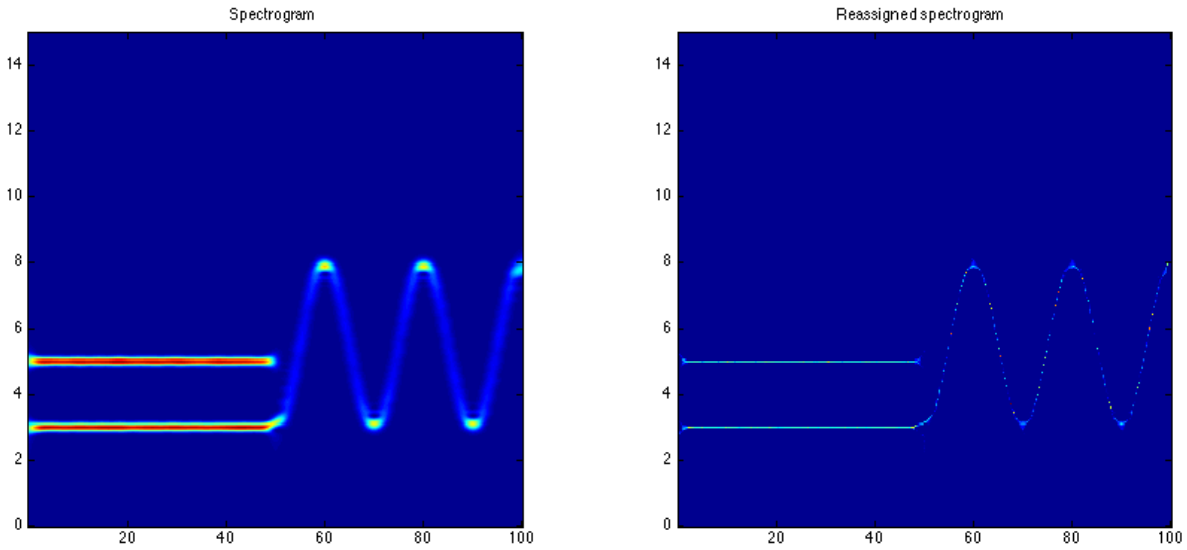

(a) Reassigned spectrogram

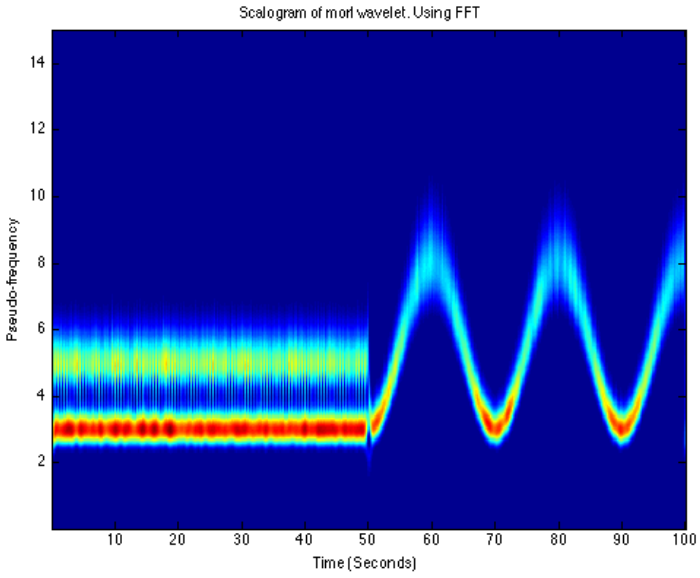

(b) Scalogram

Figure 3.14: Time frequency representations for the signal with noise level $\sigma = 0.1$.

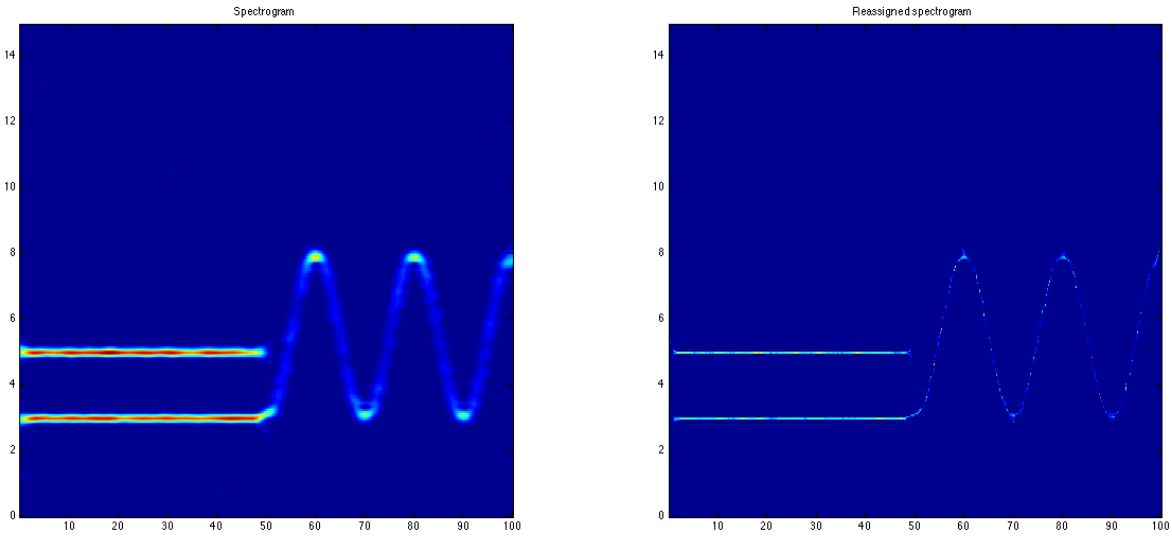

(a) Reassigned spectrogram

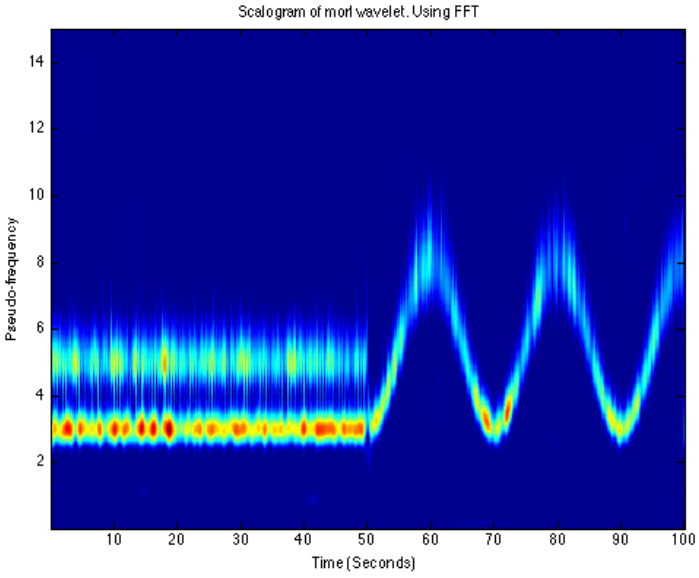

(b) Scalogram

Figure 3.15: Time frequency representations for the signal with noise level $\sigma = 0.3$.

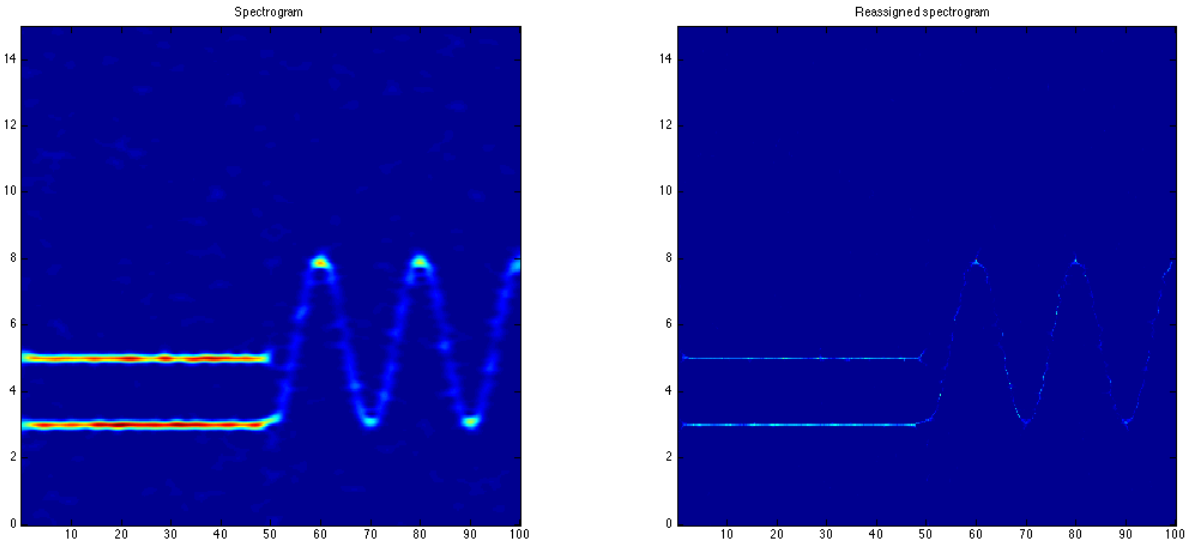

(a) Reassigned spectrogram

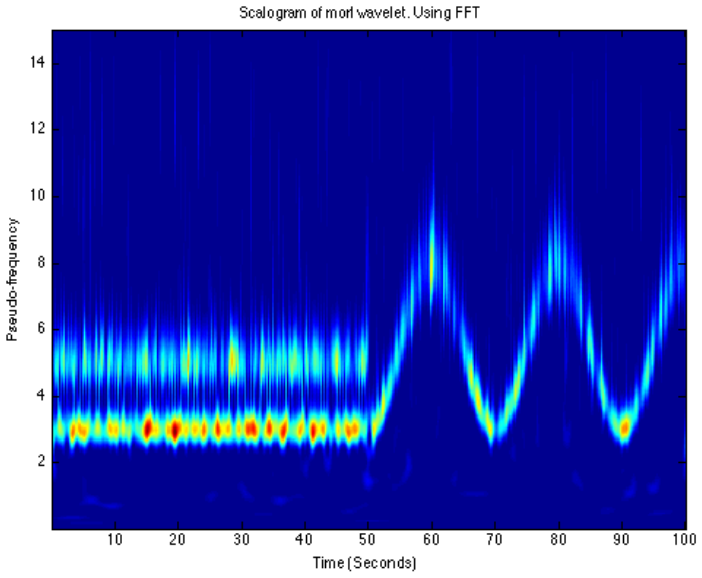

(b) Scalogram

Figure 3.16: Time frequency representations for the signal with noise level $\sigma = 0.5$.

Table 3.5: Performance measures for each method

		N_c	N_f	N_m	MSE	ρ	IF	res
$\sigma = 0.1$	**Reass. Spectrogram**	59.37	40.13	0.50	0.268	0.797	0.103	0.0001
	Scalogram	73.76	25.74	0.5	3.250	0.243	0.138	0.0133
$\sigma = 0.3$	**Reass. Spectrogram**	58.69	40.81	0.50	0.286	0.769	0.100	0.0001
	Scalogram	72.42	27.08	0.5	2.201	0.238	0.135	0.0107
$\sigma = 0.5$	**Reass. Spectrogram**	58.44	41.06	0.50	0.352	0.740	0.096	0.0002
	Scalogram	62.63	36.7	0.5	1.807	0.228	0.116	0.0116

As it can be seen from the figures and the table spectrogram reassignment surpasses scalogram in noise resistance, localization and introduces least distortions. Next chapter will show results of spectrogram reassignment on the real data.

Chapter 4

Real data analysis

4.1 Data description

Data is obtained from **6** different patients and recorded during routine anesthesia, before and after surgical incision. Each data file contains:

- 30-second recording 2.5 - 2 min before incision;
- 30-second recording 2 - 2.5 min after incision;
- 10-minute recording around incision (1-47Hz filtered). High peak at the beginning of incision because of the tap on the electrode.

Signals are obtained from prefrontal montage and sampled at 128 Hz.

Patients can be divided in two groups by:

1. anesthetic drug they received: **propofol or desflurane**;
2. whether they **had dreams or not** during operation.

Signals in time domain are presented in the following figure. Time is given in seconds, top axes contains the signal centered around incision, the bottom left axes presents 30 seconds before incision and the bottom right one – 30 seconds after.

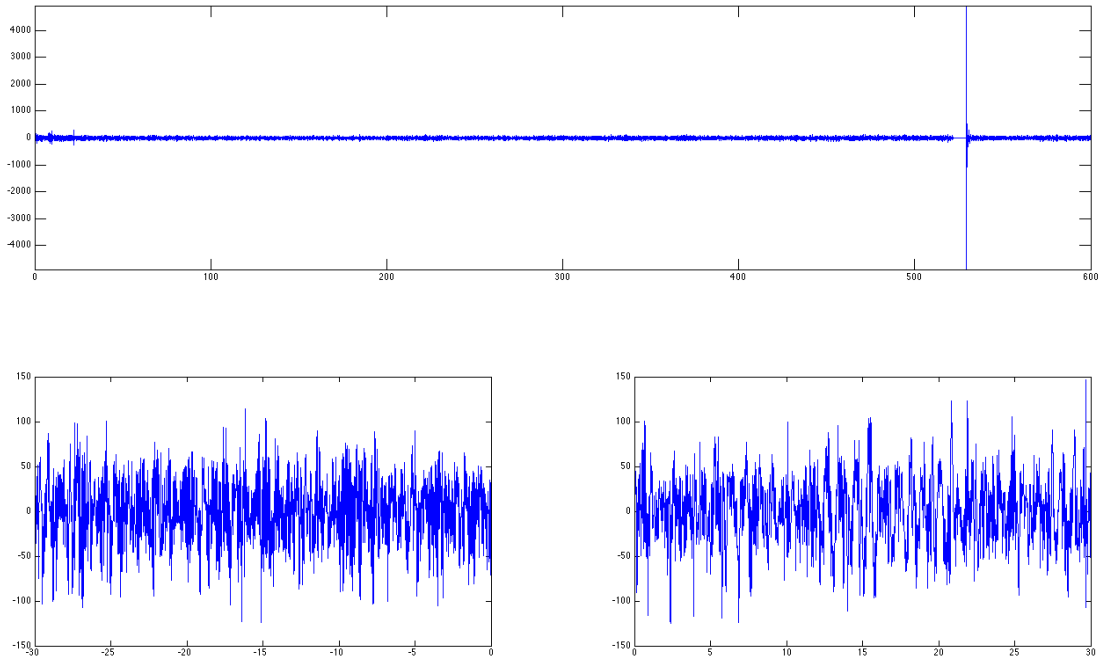

(a) Patient #1201. Propofol. Dreaming.

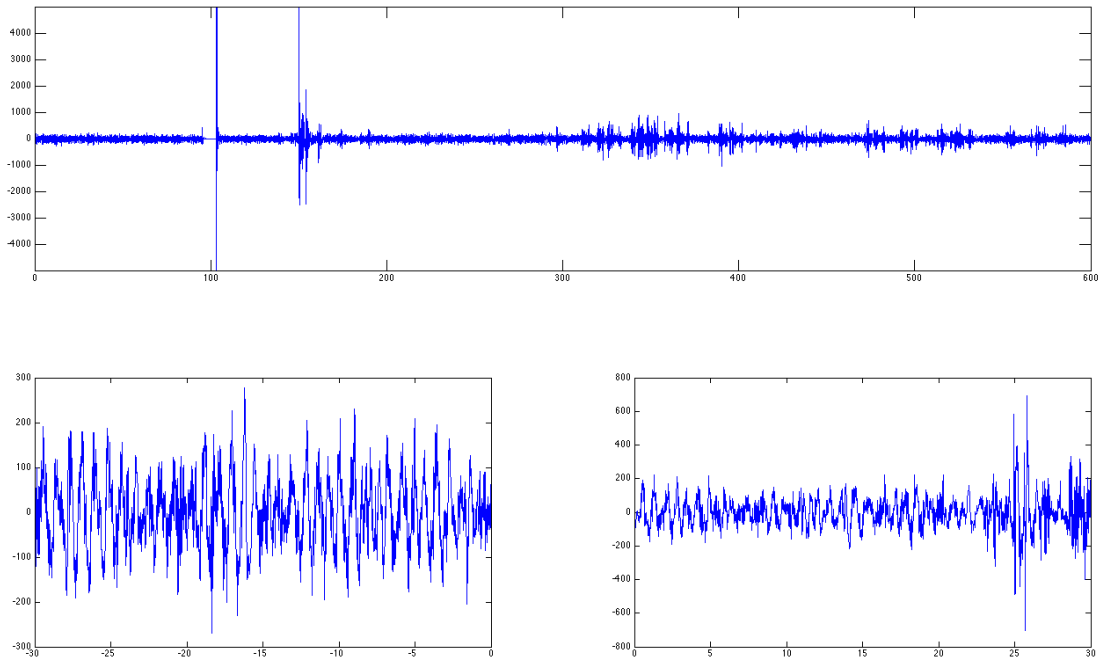

(b) Patient #1203. Desflurane. No dreaming.

Figure 4.1: Real data in the time domain. Intervals centered at, pre- and post-incision.

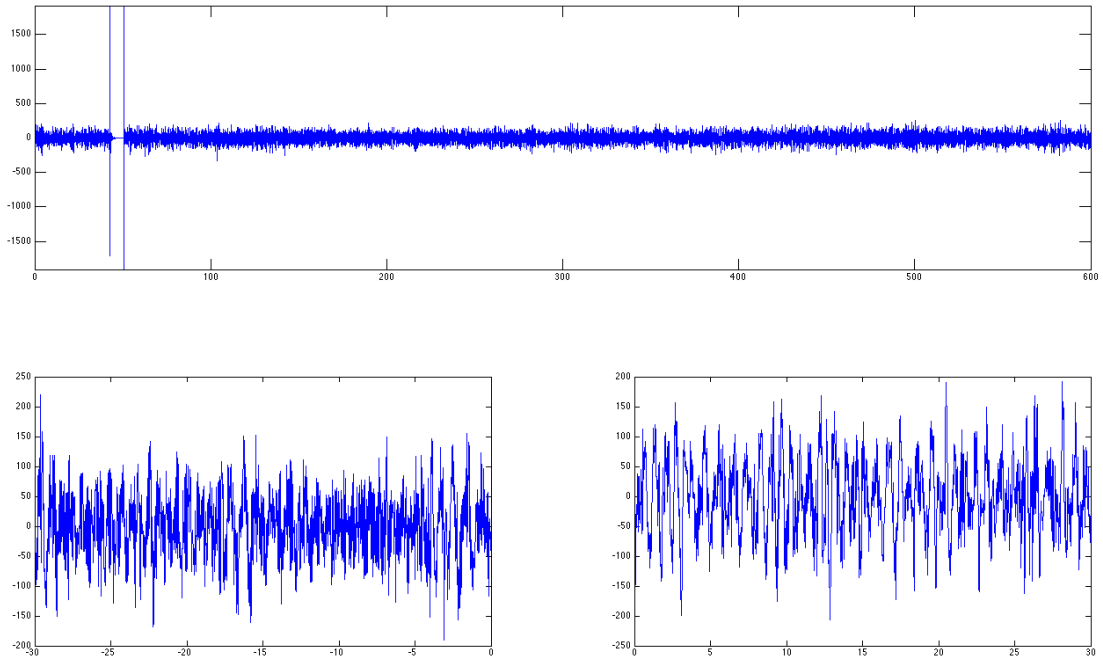

(a) Patient #4002. Propofol. Dreaming.

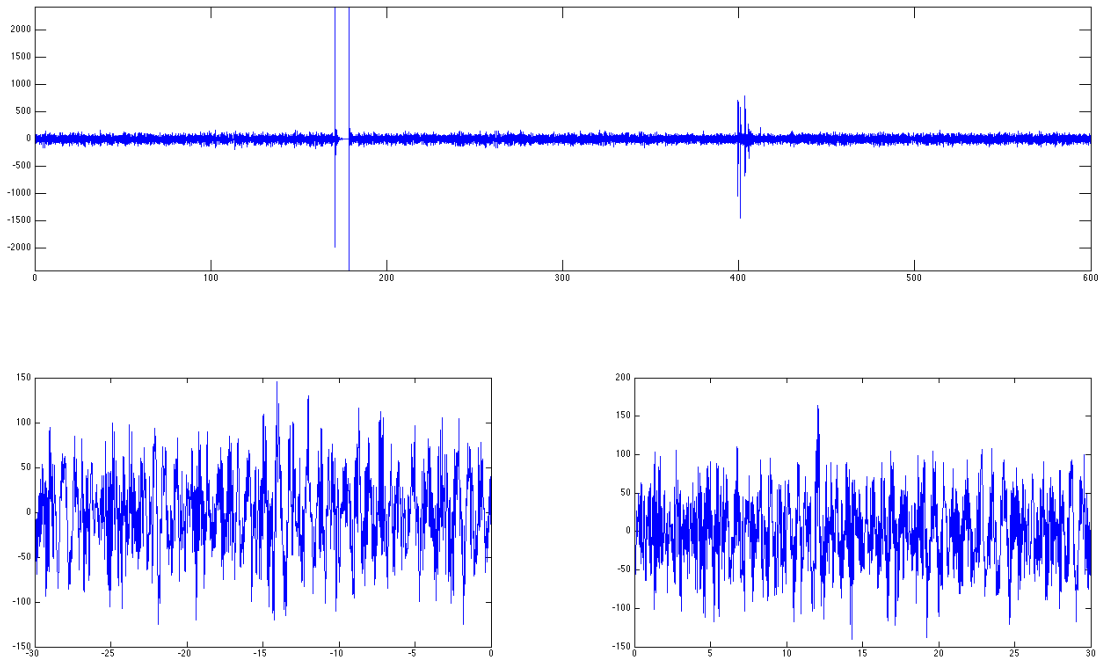

(b) Patient #4010. Desflurane. No dreaming.

Figure 4.2: Real data in the time domain. Intervals centered at, pre- and post-incision (Continued).

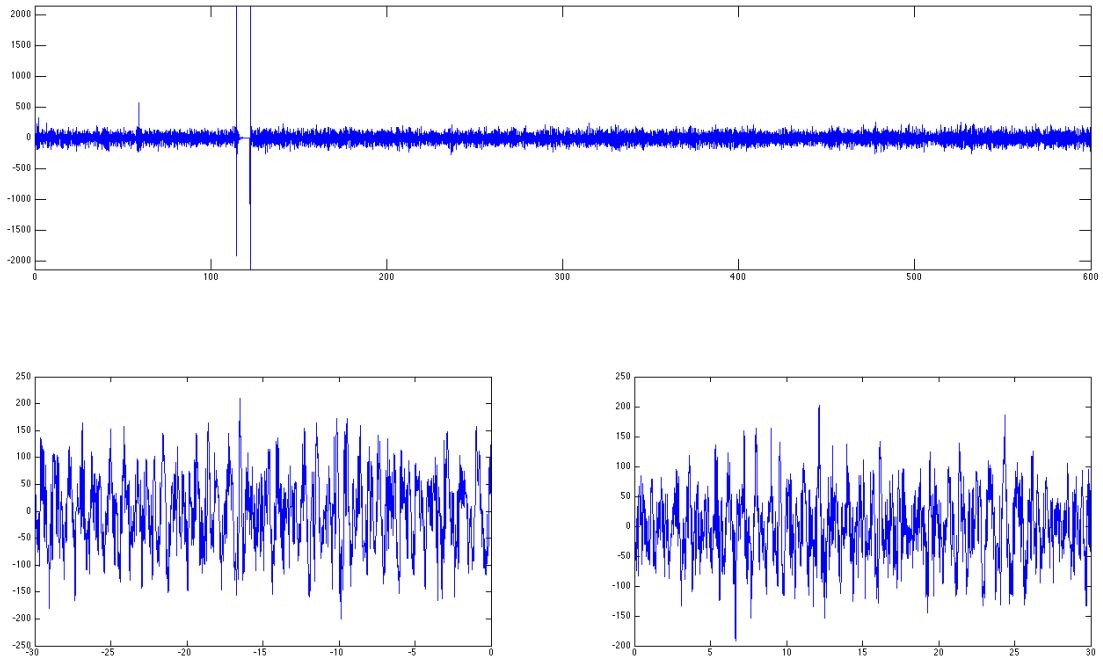

(a) Patient #4011. Propofol. No dreaming

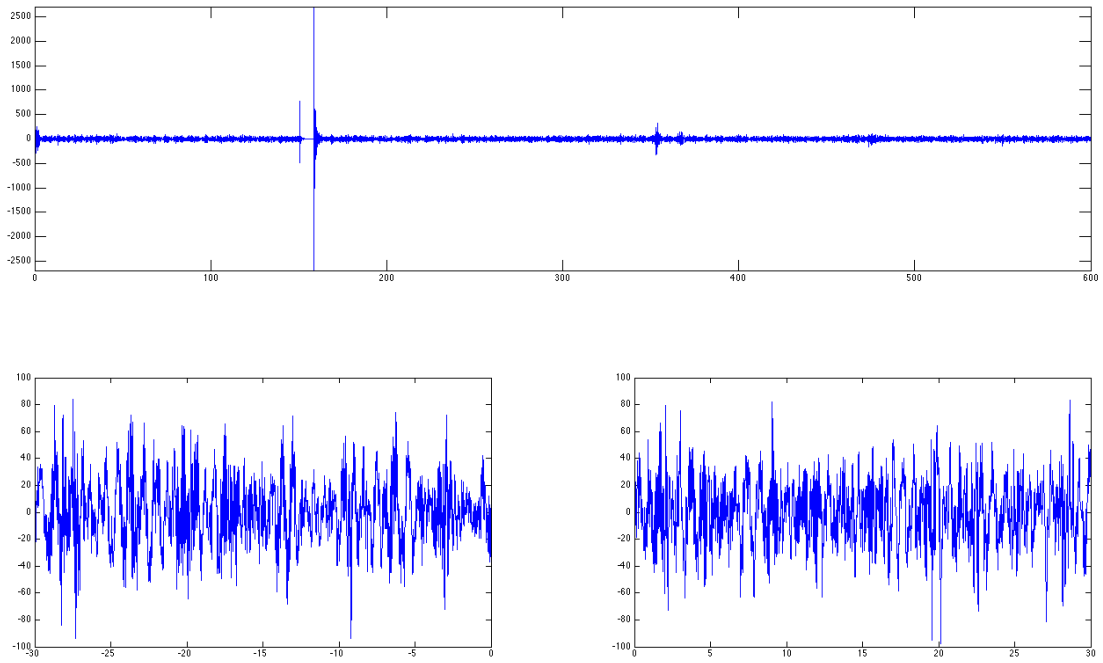

(b) Patient #4012. Desflurane. No dreaming.

Figure 4.3: Real data in the time domain. Intervals centered at, pre- and post-incision (Continued).

4.1.1 Results for real data

The time-frequency representations were obtained from the signals using method of spectrogram reassignment, it was calculated only for pre- and post-incision short intervals.

The analyzed frequencies were chosen to be from 0 Hz to 64 Hz (half of the sampling frequency) with a step of 0.1 Hz. But the signal was 1-47 Hz filtered and looking at the fig. 4.4 it can be seen that no activity is present over 30 Hz, because of that it would be more appropriate to use smaller frequency range (1-30 Hz) but with higher resolution (smaller step). Frequency step should be chosen not less than 0.05 Hz, because duration of the signal T should be more than $1/\Delta f$. Duration of the signals is 30 s, that means that $\Delta f > 1/T = 0.033$. The time-frequency representations obtained with reassigned spectrogram can be seen on the figures below.

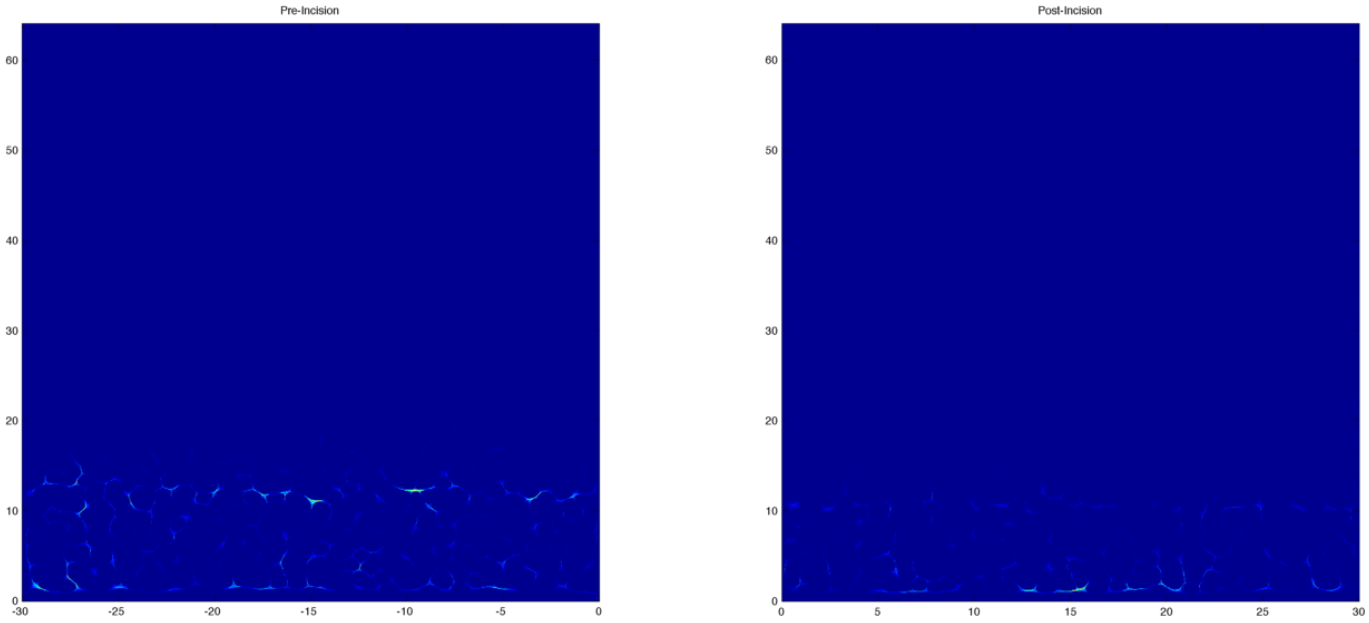

(a) Patient #1201.

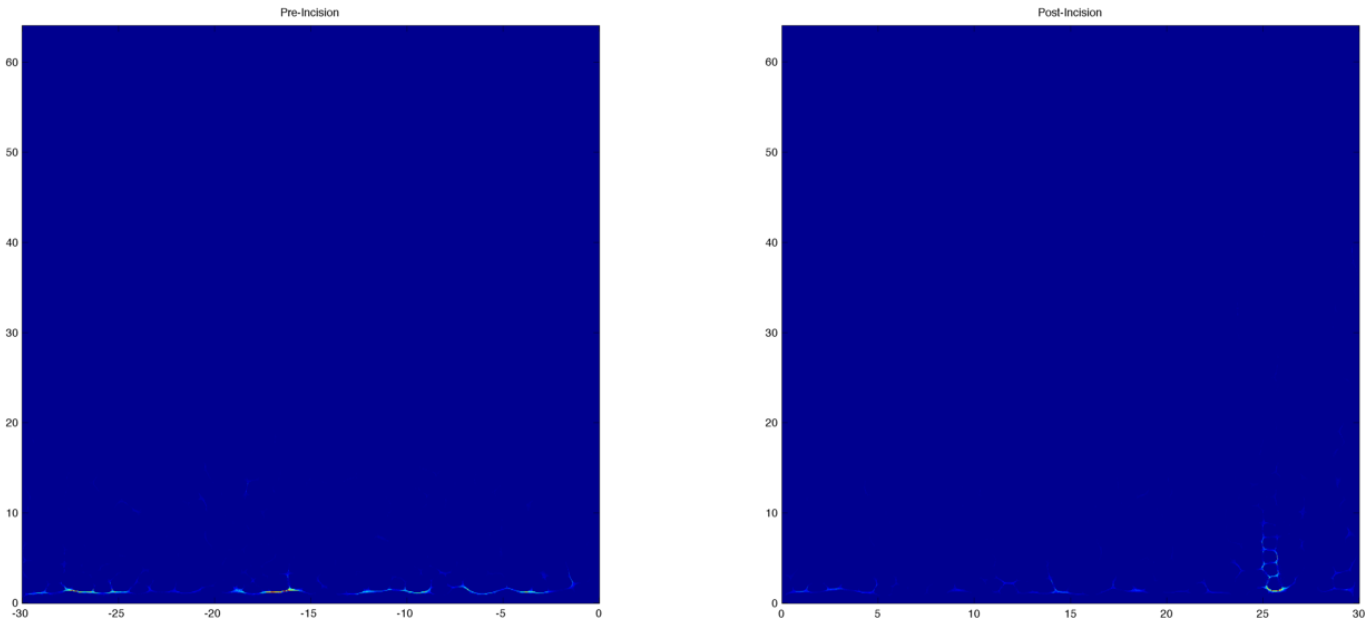

(b) Patient #1203.

Figure 4.4: Reassigned spectrograms for pre- and post-incision data.

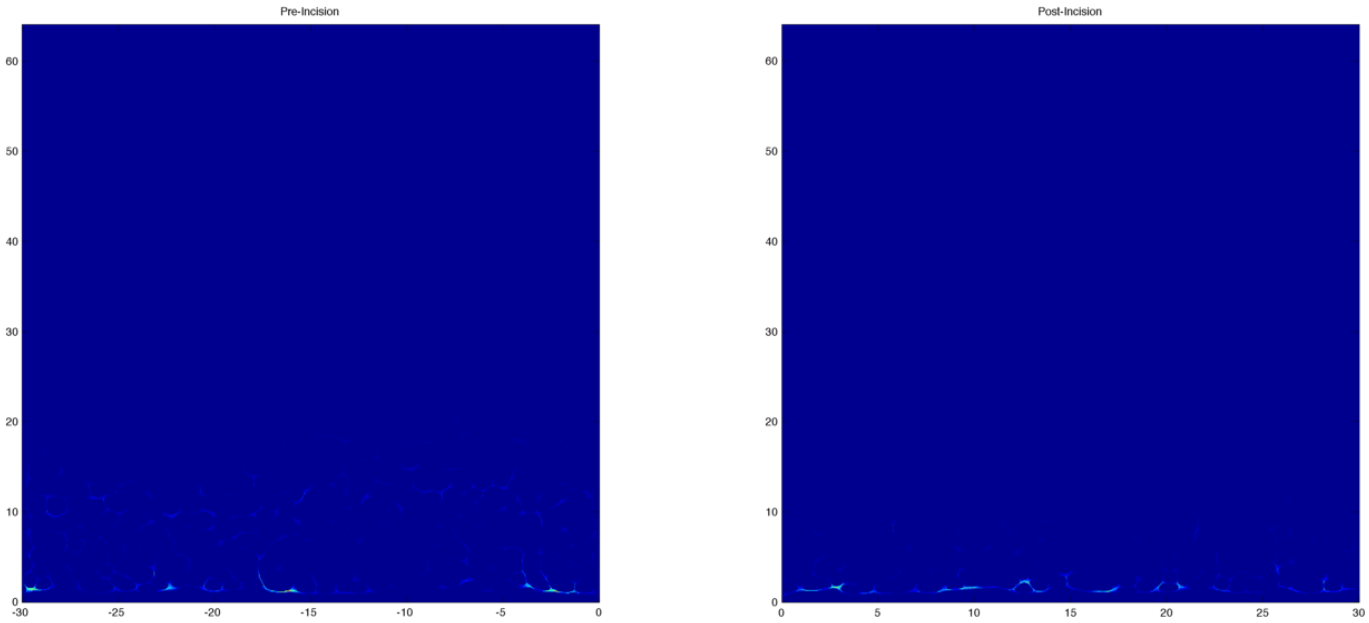

(a) Patient #4002.

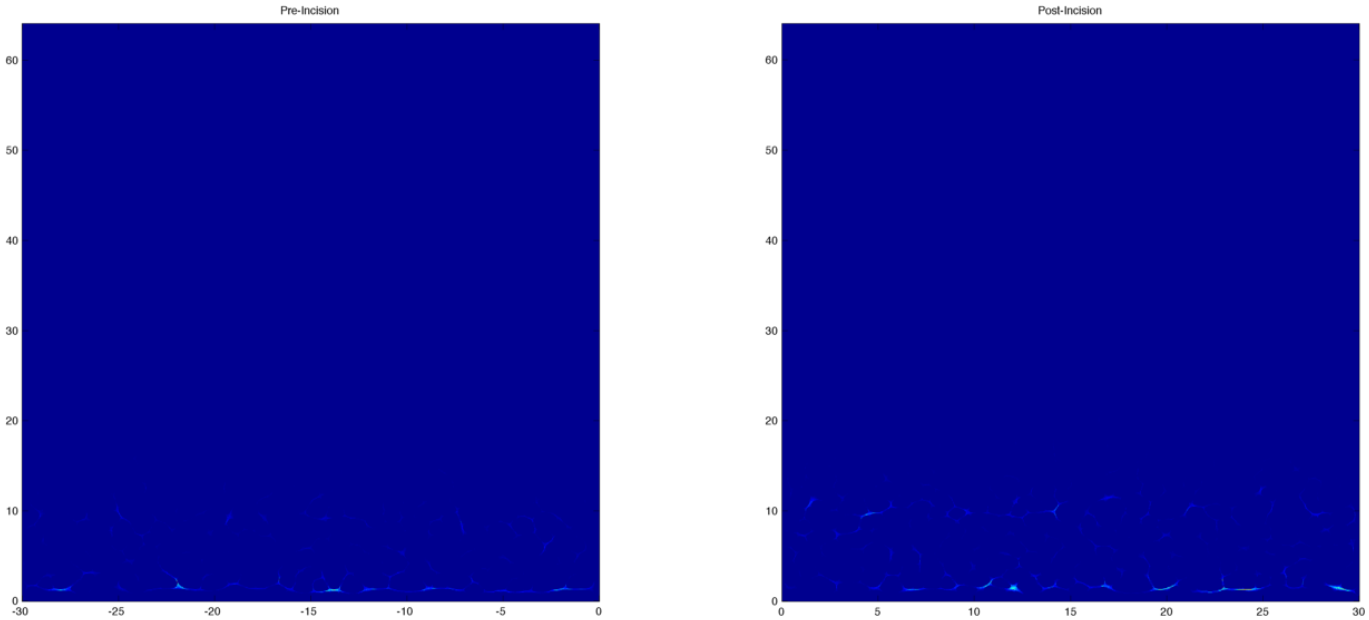

(b) Patient #4010.

Figure 4.5: Reassigned spectrograms for pre- and post-incision data (Continued).

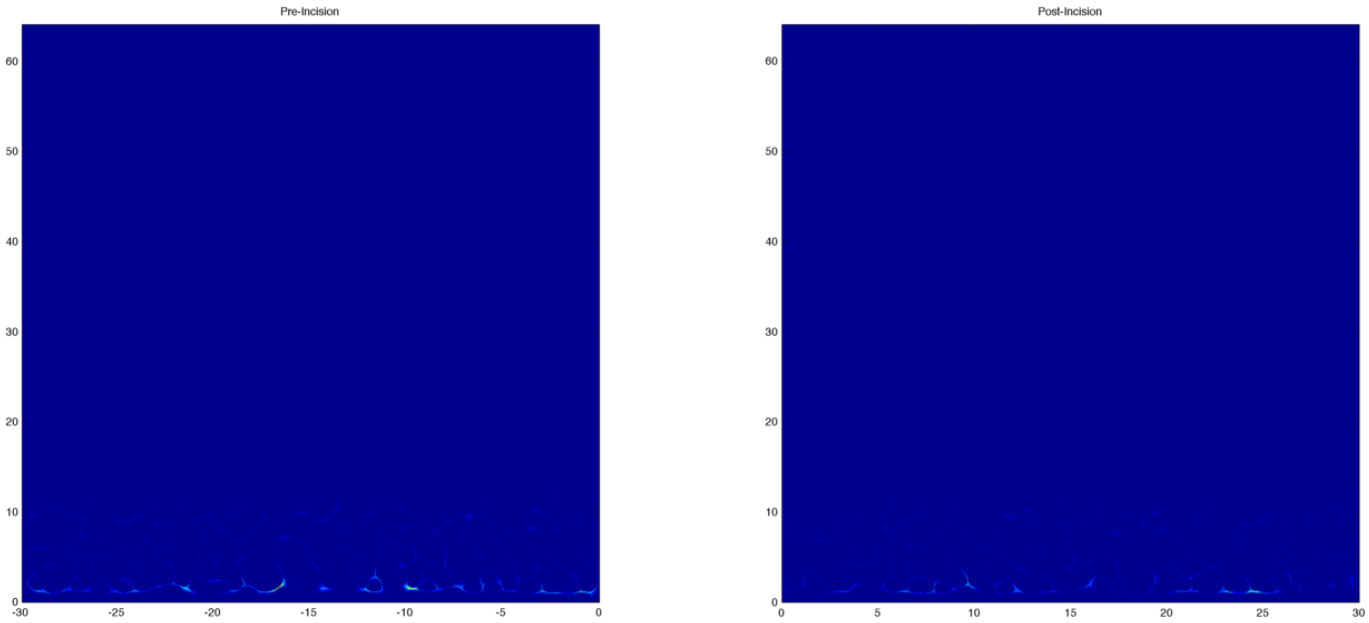

(a) Patient #4011.

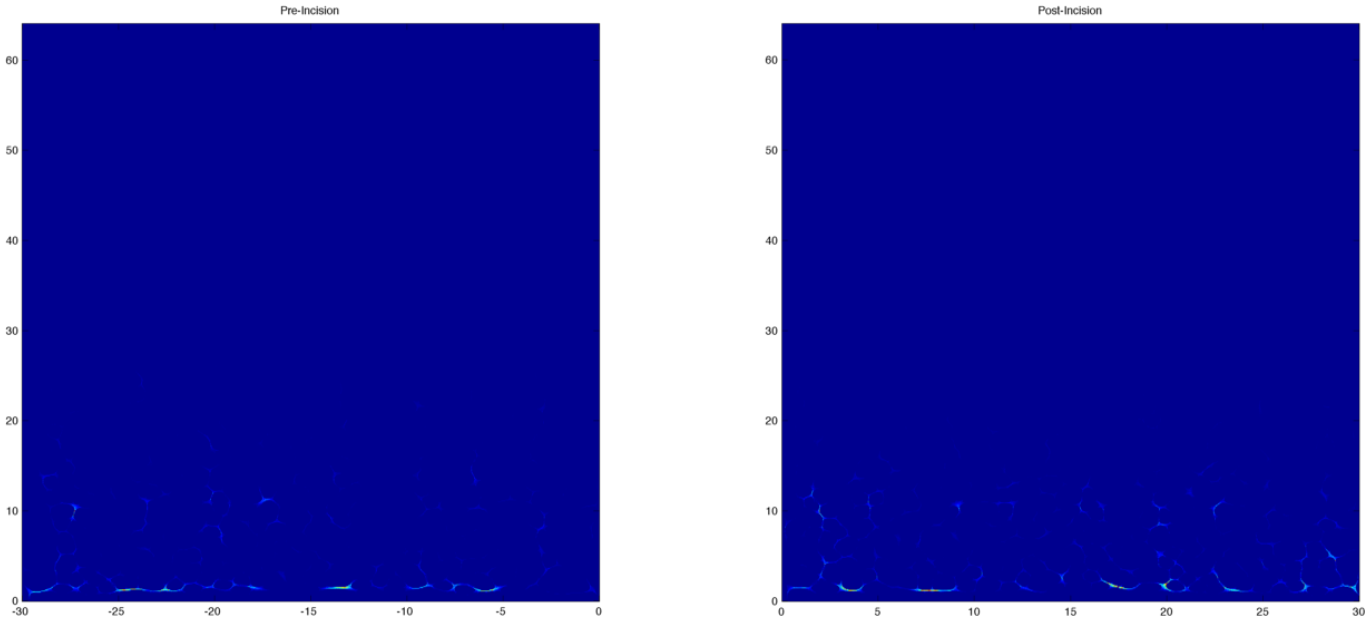

(b) Patient #4012.

Figure 4.6: Reassigned spectrograms for pre- and post-incision data (Continued).

Next, time-frequency representation was averaged over five frequency bands:

- delta: 1 – 4 Hz;
- theta: 4 – 8 Hz;
- alpha: 8 – 12 Hz;
- beta: 12 – 20 Hz;
- gamma: > 20 Hz.

The results are shown on fig. 4.7

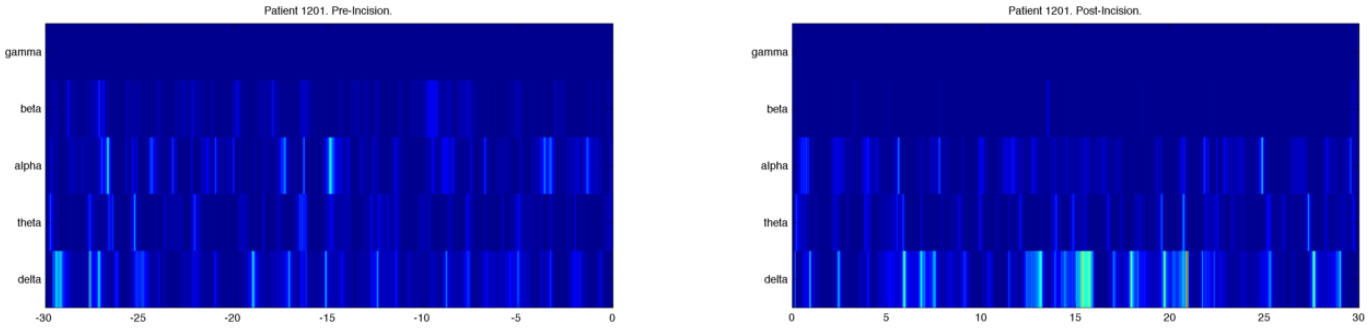

(a) Patient #1201.

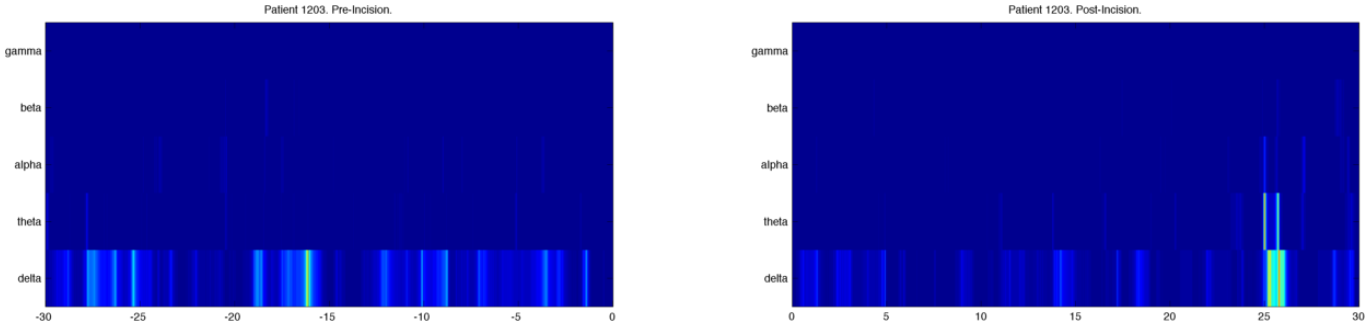

(b) Patient #1203.

Figure 4.7: Reassigned spectrograms for pre- and post-incision data. Average over frequency bands.

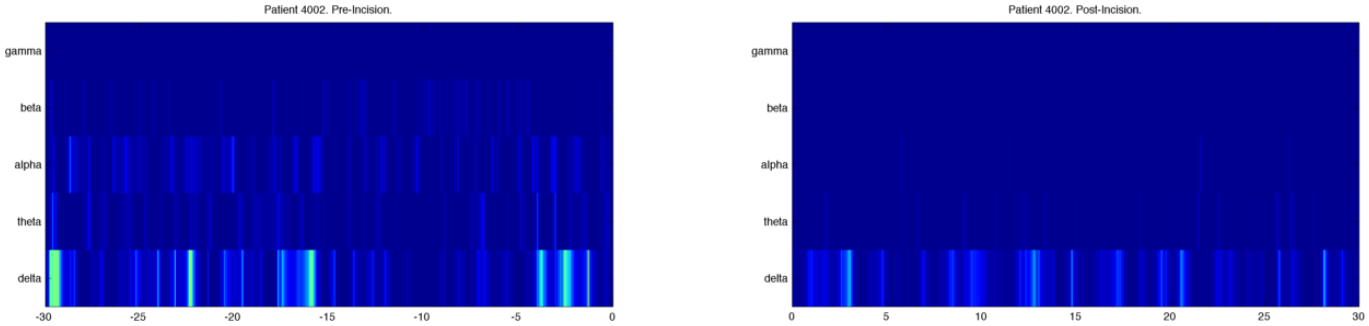

(a) Patient #4002.

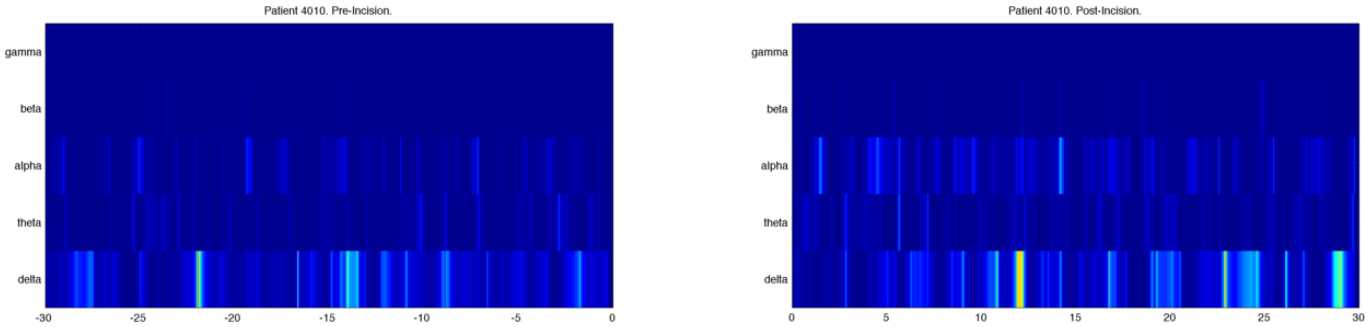

(b) Patient #4010.

Figure 4.8: Reassigned spectrograms for pre- and post-incision data. Average over frequency bands (Continued).

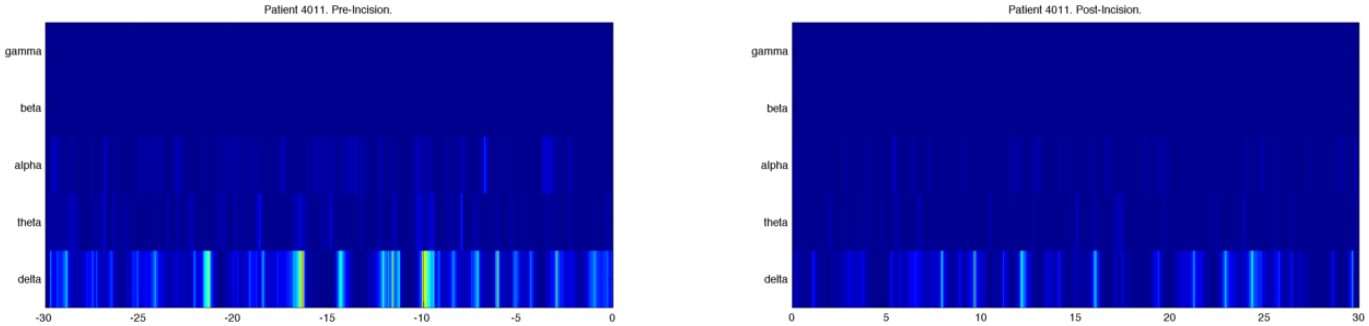

(a) Patient #4011.

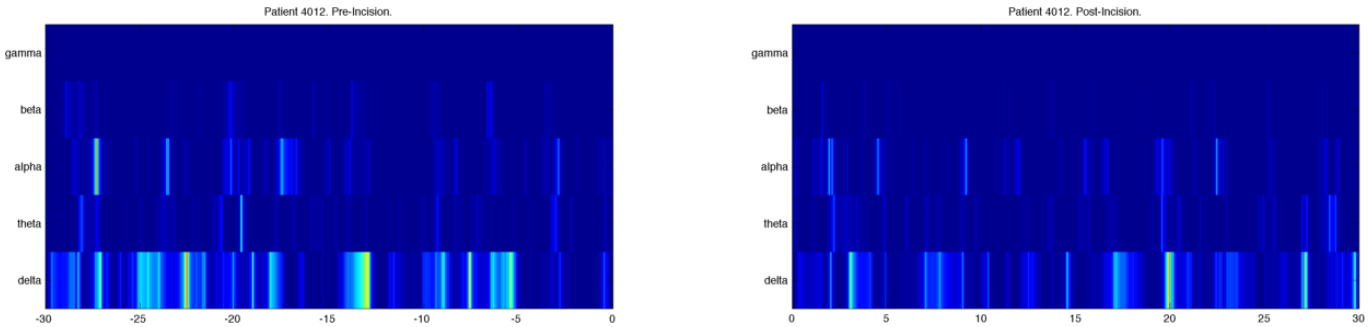

(b) Patient #4012.

Figure 4.9: Reassigned spectrograms for pre- and post-incision data. Average over frequency bands (Continued).

Chapter 5

Conclusion

Wigner-Ville and Choi-Williams distributions introduce a lot of distortions due to the interference terms and negative components. They also requires a lot of computational time.

Spectrogram better preserve energy distribution (comparing to wavelet transform), but it has issues with time/frequency resolution and gives rather rough estimates.

Wavelet transform and scalograms based on it provide good results, but add artifacts on frequencies close to zero (convolution-based method) or close to the edges (FFT-based method). Also it distorts energy distribution: high frequencies have less power comparing to lower ones. Also the TFR is blurred and it gets stronger with rise of frequency.

Frequency reassignment appears to provide indeed precise results from visual inspection. Quantitative characteristics (N_c, N_f, N_m) might have low values because most of the power on the TFR looks "reduced" comparing to certain small regions. So these regions get value 1 after normalization and the rest of frequency components are ≈ 0.5, which can be a reason of the error, since ideal TFR assumes 1 for all of the components.

Final notes:

1. Spectrogram computed by Matlab might overcome Spectrogram computed with TFTB in certain criteria, but it uses less time points, which is bad for recurrence plots.
2. Spectrograms shows better results than WV or CW distributions for this test data, because frequency components are linear, and WVD are considered to be better for nonlinear frequency laws.
3. Spectrogram reassignment was chosen as a method in future work due to:
    - good localization both in time and frequency;
    - high noise resistance;
    - least power distortions.
4. Methods which could also be studied:
    - filtered spectrogram;
    - synchrosqueezing;
    - multitapers.

Bibliography

[1] Paul S Addison. *The illustrated wavelet transform handbook: introductory theory and applications in science, engineering, medicine, and finance*. Institute of Physics Pub., Bristol, UK; Philadelphia, 2002.

[2] El H. Bouchikhi, V. Choqueuse, M. E. H. Benbouzid, J. F. Charpentier, and G. Barakat. A comparative study of time-frequency representations for fault detection in wind turbine. In *IECON 2011-37th Annual Conference on IEEE Industrial Electronics Society*, page 35843589. IEEE, 2011.

[3] Franois Auger, Patrick Flandrin, Paulo Gonalvs, and Olivier Lemoine. Time-frequency toolbox. for use with MATLAB. `http://tftb.nongnu.org/tutorial.pdf`, 1996. Accessed: 2014-03-31.

[4] Douglas L. Jones and Thomas W. Parks. A resolution comparison of several time-frequency representations. *Signal Processing, IEEE Transactions on*, 40(2):413420, 1992.

[5] Luke Rankine, Nathan Stevenson, Mostefa Mesbah, and Boualem Boashash. A quantitative comparison of non-parametric time-frequency representations. In *Proc. European Conf. on Signal Processing, Antalya, Turkey*, 2005.

[6] Thayananthan Thayaparan. Linear and quadratic time-frequency representations. Technical report, DTIC Document, 2000.

[7] Christopher Torrence and Gilbert P. Compo. A practical guide to wavelet analysis: `http://paos.colorado.edu/research/wavelets/`. *Bulletin of the American Meteorological Society*, 79:61–78, 1998.

[8] Zhou Wang and A.C. Bovik. Mean squared error: Love it or leave it? a new look at signal fidelity measures. *IEEE Signal Processing Magazine*, 26(1):98–117, January 2009.